


Cell membrane-camouflaged PLGA biomimetic system for diverse biomedical application

Jingjing Yan[#], Weidong Fei[#], Qianqian Song, Yao Zhu, Na Bu, Li Wang, Mengdan Zhao  and Xiaoling Zheng

Department of Pharmacy, Women's Hospital, Zhejiang University School of Medicine, Hangzhou, China

ABSTRACT

The emerging cell membrane (CM)-camouflaged poly(lactide-co-glycolide) (PLGA) nanoparticles (NPs) (CM@PLGA NPs) have witnessed tremendous developments since coming to the limelight. Donning a novel membrane coat on traditional PLGA carriers enables combining the strengths of PLGA with cell-like behavior, including inherently interacting with the surrounding environment. Thereby, the *in vivo* defects of PLGA (such as drug leakage and poor specific distribution) can be overcome, its therapeutic potential can be amplified, and additional novel functions beyond drug delivery can be conferred. To elucidate the development and promote the clinical transformation of CM@PLGA NPs, the commonly used anucleate and eukaryotic CMs have been described first. Then, CM engineering strategies, such as genetic and nongenetic engineering methods and hybrid membrane technology, have been discussed. The reviewed CM engineering technologies are expected to enrich the functions of CM@PLGA for diverse therapeutic purposes. Third, this article highlights the therapeutic and diagnostic applications and action mechanisms of PLGA biomimetic systems for cancer, cardiovascular diseases, virus infection, and eye diseases. Finally, future expectations and challenges are spotlighted in the concept of translational medicine.

Abbreviations: AS: atherosclerosis; BBB: blood-brain barrier; CCM: cancer cell membrane; Ce6: chlorin e6; CM@PLGA NPs: cell membrane-camouflaged PLGA nanoparticles; CTLs: cytotoxic T lymphocytes; Cur: curcumin; CXCR4: C-X-C chemokine receptor type 4; DC: dendritic cell; DOX: doxorubicin; EC: endothelial cell; FL: fluorescence; HUVEC: human umbilical vein endothelial cell; ICG: indocyanine green; LPS: lipopolysaccharide; MM: macrophage membrane; MRI: magnetic resonance image; MSC: mesenchymal stem cell; NSC: neural stem cell; NIR: near-infrared; PA: photoacoustic; PLGA NPs: poly(lactide-co-glycolide) nanoparticles; PM: platelet membrane; PFP: perfluoropentane; PTX: paclitaxel; RA: rheumatoid arthritis; RBC: red blood cell; RBCM: red blood cell membrane; SC: stem cell; TAAs: tumor associated antigens; TAM: tumor-associated macrophages; TCR: T-cell receptor; TME: tumor microenvironment; TRAIL: tumor necrosis factor-related apoptosis-inducing ligand; UC: ulcerative colitis; US: ultrasounds; VEGF: vascular endothelial growth factor; VCAM-1: vascular cell adhesion molecule-1

ARTICLE HISTORY

Received 1 June 2022
Revised 29 June 2022
Accepted 4 July 2022





KEYWORDS

Cell membrane; PLGA; membrane vesicles engineering; biomimetic; application

1. Introduction

Biodegradable polymers are well-established as a mainstay in the realm of biomedical applications owing to their versatility and flexible engineering strategies. Among the numerous nanocarriers, PLGA possesses attractive superiority and has been featured in a substantial number of publications and preclinical studies since its discovery. In the field of medical science, PLGA was developed as a material for biodegradable sutures in the 1970s, followed by its use in the production of devices such as implants, tissue grafts, prosthetic devices, and therapeutic devices. Presently, the technology has matured to the nanoscale. Poly(lactide-co-glycolide) (PLGA) (MW: 4–240 kDa) has been used for the encapsulation

of various types of drugs, such as paclitaxel (PTX), doxorubicin (DOX), cisplatin, docetaxel, and curcumin (Cur) (Swider et al., 2018). The FDA has so far approved approximately 20 PLGA-based formulations for use in several indications, such as oncology, mental illness, and osteoarthritis (Park et al., 2019; Allen & Evans, 2020). PLGA is polymerized from lactic acid and glycolic acid. Monomers of lactic acid and glycolic acid are easily decomposed into carbon dioxide and water via the tricarboxylic acid cycle (Pandita et al., 2015). The key merits of PLGA are biocompatibility, tunable biodegradation rate, mechanical strength, surface flexibility for modification, tolerance to loading a wide range of drugs, and sustained payload release (Park et al., 2019). Of note, these properties largely depend on the physicochemical characteristics of

CONTACT Mengdan Zhao  dreamdan@zju.edu.cn  Department of Pharmacy, Women's Hospital, Zhejiang University School of Medicine, Hangzhou 310006, China; Xiaoling Zheng  ekwefi@zju.edu.cn  Department of Pharmacy, Women's Hospital, Zhejiang University School of Medicine, Hangzhou 310006, China.

[#]These authors contributed equally to this work.

© 2022 The Author(s). Published by Informa UK Limited, trading as Taylor & Francis Group.

This is an Open Access article distributed under the terms of the Creative Commons Attribution-NonCommercial License (<http://creativecommons.org/licenses/by-nc/4.0/>), which permits unrestricted non-commercial use, distribution, and reproduction in any medium, provided the original work is properly cited.

PLGA. For example, researchers could achieve a desired degradation rate and drug release rate by controlling the relevant parameters, such as polymer molecular weight, the ratio of lactide to glycolide, and the formulation method (Makadia & Siegel, 2011).

Despite the above advantages, PLGA has some major drawbacks, such as initial burst release, poor biodistribution, rapid phagocytic clearance, and short circulation half-life that hinder its clinical usage. Several commonly used techniques have been reported, such as PEGylation and targeting ligand modification. PEGylation, a well-established technique, has been used to make NPs hydrophilic and stealth to protect them from immune clearance. However, many clinical studies have demonstrated that the appearance of anti-PEG antibodies can result in faster blood clearance, allergies, or even life-threatening complications (Thi et al., 2020). An unexpected negative effect of PEGylation on erythrocytes is impaired deformability, oxygen transport capacity, and thus, potential organ dysfunction (de la Harpe et al., 2019). Moreover, the targeted ligand grafting process requires a series of chemical conjugation steps and labor-intensive work. Additionally, the organic solvents and highly reactive chemical reagents used to obtain the target nanocomposite are not environmentally friendly. Our group was devoted to the modification of PLGA by introducing hydrophilic groups for adjusting the synthetic hydrophobic surface, mannosylation to induce receptor-mediated endocytosis, and so forth (Zheng et al., 2010; Zhu et al., 2019). Nevertheless, the complex modification process tends to affect the industrial feasibility and druggability of PLGA-based preparations. Hence, more feasible strategies are needed to overcome the shortcomings of PLGA without affecting its clinical applications.

The advent of biomimetic nanotechnology ushers in a new era of novel nanotherapeutics for effective disease intervention. Since Hu et al. (2011) pioneered the invention of erythrocyte membrane-wrapped PLGA biomimetic NPs, cell membrane (CM)-derived drug delivery systems have expanded rapidly in the medical field. Nature-inspired nanotherapeutics integrate the advantages offered by the rich functionalities of natural CMs and the engineering flexibility of synthetic materials to form functional nanostructures. From a biological standpoint, the outer shell of CM-camouflaged PLGA nanoparticles (NPs) (CM@PLGA NPs) possesses complex antigenic information and surface properties akin to those of original cells. Thus, CM@PLGA NPs imitate the natural cells to navigate the blood system, homologous target, and immune escape. In terms of physical properties, CM cloaking can restrain the initial burst release of cargos in circulation and enhance the dispersibility and stability in aqueous medium via increased surface potential and ideal particle size (Gou et al., 2021). Furthermore, the 'top-down' fabrication approach exempting labor-intensive procedures and chemical reagents, thus, is more eco-friendly (Dash et al., 2020).

During the past decade, CM@PLGA biomimetic systems have been applied to treat diverse diseases, such as cancer, cardiovascular, and cerebrovascular diseases, and even the ongoing severe acute respiratory syndrome coronavirus-2 (SARS-CoV-2) pandemic (Table 1). The reason why PLGA is

the starting point and often selected as the core inside the CM among many available carriers is not only its biocompatibility and biodegradability but also its physical rigidity (Makadia & Siegel, 2011), which can provide definite support for the phospholipid layer. The outer CM is not easily deformed or ruptured under the support of PLGA, thereby ensuring drug delivery to the target area. In the past decade, this field has progressed rapidly and widely. However, few comprehensive reviews spotlighting this technology and its clinical application potential have been published. Thus, there is an urgent need to outline the comprehensive design, application, and action mechanism of CM@PLGA biomimetic systems. This review presents the information on CM uncovered so far and emphasizes the surface engineering strategies for modified membrane vesicles. More importantly, this review highlights their therapeutic and diagnostic potentials in different diseases and the underlying mechanisms (Figure 1).

2. Various cell membranes

Different source cells are used to camouflage NPs including anucleate cells, prokaryotes, and eukaryotes, which confer NPs with source cells imitated biointerfacing functions. With regard to prokaryotes, bacterial outer membrane vesicles containing peptide immunogens are leveraged for antibacterial immunity (Anwar et al., 2021). However, because of the need to remove peptidoglycan, bacterial membrane extraction is tedious. Thus, the discussion of the prokaryotic membrane is not within the scope of this review. This section describes the characteristics of different CMs, which can be used as a reference for selecting suitable CMs for treating various diseases.

2.1. Anucleate cells

Erythrocytes or red blood cells (RBCs) are the most numerous blood cells in the systemic circulation. In the last century, researchers have developed RBC-based drug carriers via encapsulation or adsorption onto membranes (Mao et al., 2021). The red blood cell membrane (RBCM) possesses the merits of RBC, especially long circulation time and biocompatibility. The transmembrane protein CD47, which is a self-marker, presents 'do not eat me' signals to phagocytes (Oldenburg et al., 2000). Moreover, a dense coat of polysaccharides, called 'glycocalyx', exhibits spatial stability and also plays a vital role in immune escape. By harnessing the biocompatibility of RBCM coating on PLGA NPs, the acute inflammatory response of the biomaterial scaffold can be eliminated (Fan et al., 2018). Compared with PEGylation, RBCM derived-NPs have twice the cycle time (39.6 h vs. 15.8 h) (Hu et al., 2011). However, the disadvantages of RBCM coating technology are lack of targeting and weak tissue penetration, which inspired scientists to develop other biofilms.

Platelets are the first responders to damage and possess various physiological functions, such as hemostasis and maintenance of vascular integrity. Furthermore, platelets are essential effector cells involved in the inflammatory response and

Table 1. The classification of cell membrane camouflaged-PLGA biomimetic system for disease therapy and diagnosis.

Applications	Classification	CM source	Membrane extraction	Coating method	Cargos	Treatment outcome	Ref
Cancer	Chemotherapy	RBC	Sonication	Sonication	DOX	Immunocompatibility and advantageous safety profile; enhanced delivered DOX to lymphoma	Luk et al. (2016)
		RBC	Hypotonic lysis	Extrusion	Obatodax mesylate	Prolonged circulation time; induced apoptosis by downregulating Bcl-2	Chen et al. (2020b)
		RBC	Hypotonic lysis	Extrusion	Gambogic acid	Improved anti-colorectal cancer efficacy with good safety	Zhang et al. (2017)
		RBC	Hypotonic lysis	Sonication and extrusion	TPGS and Cur	Porous PLGA accelerated drug release	Xie et al. (2019)
		H1975 cells	Extrusion	Extrusion	DOX + Icotinib	Overcome drug resistance in EGFR-mutated lung cancer; 87.56% anti-tumor rate	Wu et al. (2019b)
		RAW264.7-4T1	Membrane protein extraction kit + sonication	Sonication	DOX	Targeted lung metastasis from breast cancer; 88.9% anti-metastasis efficacy	Gong et al. (2020)
		143B-RAW264.7	Isolation buffer + ultrasound	Extrusion	PTX	Osteosarcoma target with minimal damage to normal tissues	Cai et al. (2022)
		RBC	Hypotonic lysis	Sonication	Cyclopamine, PTX	Disrupted tumor extracellular matrix; improve tumor perfusion; improved PTX delivery	Jiang et al. (2018)
		MSC	Sucrose gradient Centrifugation	Sonication	DOX	Enhanced cellular uptake and tumor-homing with remarkable tumor growth inhibition	Yang et al. (2018)
		HeLa cells	Hypotonic lysis	Extrusion	PTX, siRNA-E7	Immune escape and tumor homing; chemo-gene combined therapy for cervical cancer	Xu et al. (2020)
		HepG2 cells	Hypotonic lysis	Sonication	DOX	Homotypic targeting; tumor volume decreased by approximately 90%	Sun et al. (2020b)
		MCF-7 cells	Hypotonic lysis + sonication	Extrusion	Hemoglobin, DOX	Broke hypoxia-induced chemoresistance	Tian et al. (2017)
		PEGylation TE10 cell	Freeze-thaw	Sonication	DOX and Cur	Inhibited the growth of DOX-resistant esophageal carcinoma; high biosafety	Gao et al. (2021)
		T-cells 19LF6	Hypotonic lysis	Extrusion	Trametinib	TCR concentration-dependent cell uptake toward the melanoma cells	Yaman et al. (2020)
		RBC	Hypotonic lysis + extrusion	Extrusion	Euphorbia factor L1	Penetrated the BBB synergistically targeted glioma cells	Cui et al. (2020)
anti-EGFR-IRGD modified RBCM	Hypotonic lysis + sonication	Extrusion	Gambogic acid	Improved tumor targeting ability	Zhang et al. (2018b)		
T7 modified RAW 264.7	Hypotonic lysis + extrusion	Extrusion	Saikosaponin D	Inhibited tumor growth and lung and spleen metastasis of breast cancer	Sun et al. (2020a)		
TRAIL modified HUVECs	Lysis	Extrusion	Oxallipatin,	Inhibited autophagy, reversed focal adhesion disassembly and attenuated metastasis	Shi et al. (2021)		
Galactose-inserted RBCM	Hypotonic lysis	Extrusion	Baicalin, Hgp 100 ²⁵⁻³³ + CpG	Enhanced tumor targeting and reversed TAM phenotype for immune activation	Han et al. (2019)		
U87; MDA-MB-231; BT474	Homogenize; gradient centrifugation; extrusion	Extrusion	/	Reduced the ability of fibroblasts to attract cancer cells; induced an immune response	Jin et al. (2019)		
T cell line (EL4 cells)	Hypotonic lysis + sonication	Sonication	Dacarbazine	Restored cytotoxic functions of CTLs; antigen-nonspecifically eradicated tumor	Kang et al. (2020)		
PEI-modified macrophages	Membrane protein extraction kit + freeze-thaw	Extrusion	Dendrobium polysaccharides, OVA	Positive charge promoted antigen uptake; stimulated humoral and cellular immunity	Zhang et al. (2020b)		
DC-tumor fusion cells	Hypotonic lysis + freeze-thaw	Extrusion	CpG	Penetrated immune organs and activated T cells; repressed peripheral tumors or glioma	Ma et al. (2020)		
DC-tumor fusion cells	Hypotonic lysis + freeze-thaw	Extrusion	CpG ODN	Strong immune activation; inhibited allograft, xenograft and metastatic tumor	Zhang et al. (2022b)		
LPS-treated macrophage	Sucrose gradient centrifugation	Extrusion	Fe ₃ O ₄ , R837	Activated IRF5 or NF-κB signaling pathway; polarized TAMs from M2 to M1 phenotype	Liu et al. (2020a)		
RAW 264.7 cells	Low osmotic + ultrasound	Extrusion	DOX	Enhanced ICD and antigen presentation by combining with XCL-1 loaded in situ gel	Xiong et al. (2021)		
4T1 cells	Hypotonic lysis	Extrusion	Imiquimod	Activated the immune system and established immune memory	Xiao et al. (2021)		
CBP-12 modified B16-OVA-TC1, 4T1	Membrane protein extraction kit + extrusion	Extrusion	2'-3'-cGAMP STING agonist	Delivered both TAAs and STING agonists to Clec9a ⁺ DC; increased proliferation of naïve T cells	Gou et al. (2021)		
KPC	Hypotonic lysis + freeze-thaw	Extrusion	Gemcitabine	M2pep and TAAs were capable of TAM and cancer targeting and TME reprogram	Wang et al. (2022a)		
Folic acid modified RBCM	Hypotonic lysis + centrifugation	Extrusion	DOX, ICG	pH-dependent and NIR-triggered drug release; synergistic chemo-PTT antitumor efficacy	Chen et al. (2021)		
MCF-7 cells	Hypotonic lysis	Sonication	ICG-10, DOX, Mcl-1-siRNA	NIR and pH triggered release; magnetic and homotypic homing; overcome chemoresistance	Guo et al. (2022)		
MCF-7 cells	Hypotonic lysis + mechanical disruption	Extrusion	Cur and C66	Homologous tumor targeting; PDT combined with chemotherapy	Zhang et al. (2021)		
Human osteosarcoma cells	Membrane and cytosol protein extraction kit	Extrusion	IR780	Homologous targeting-associated PDT with apoptosis and ferroptosis death mode	Wang et al. (2022b)		
platelet	Freeze-thaw	Sonicate	ICG	X-ray pretreatment further enhanced endocytic in 4T1 breast cancer cell	Chen et al. (2020c)		
Hyaluronidase modified RBCM	Hypotonic lysis and extrusion	Extrusion	/	Stable enzyme anchorage and reservation of its enzymatic activity without RBCM destruction	Zhou et al. (2016)		
RBC	Hypotonic treatment	Extrusion	Perfluorocarbon	Relieved tumor hypoxia by deliver oxygen into tumors; enhanced cancer radiotherapy	Gao et al. (2017b)		
RBC	Hypotonic treatment and extrusion	Extrusion	Glucose oxidase, Mn ₂ (CO) ₁₀	Synergistic efficacy of starvation therapy and CO gas therapy	Wang et al. (2019c)		

(Continued)

Table 1. Continued.

Applications	Classification	CM source	Membrane extraction	Coating method	Cargos	Treatment outcome	Ref
Inflammation	AS	MM	Membrane protein extraction kit	Extrusion	Rapamycin	Active targeted activated ECs; significantly delayed the progression of AS	Wang et al. (2021)
Stroke	MM	CD47 and integrin modified	Hypotonic lysis	Extrusion	Colchicine	Targeted inflammatory ECs while avoiding endocytosis by macrophages	Li et al. (2022)
		CXCR4-mouse NSCs	Hypotonic lysis + freeze-thaw process	Extrusion	Glyburide	Enhanced delivery of NPs to the ischemic brain and augment efficacy of glyburide	Ma et al. (2019)
RA	Neutrophil	TRAIL-HUVEC	Hypotonic lysis	Sonication	/	Decoys of neutrophil-targeted biomolecules; synovial inflammation and joint damage inhibition	Zhang et al. (2018a)
UC	Sepsis	TLR4-MM	Repeated freeze-thaw	Extrusion	Tasquinimod	Orally targeted colitis drug delivery system	Li et al. (2021c)
		Murine J774 cell	Hypotonic lysis + mechanical disruption	Sonication	/	Acted as a LPS and cytokine decoy	Thamphiwatana et al. (2017)
Detoxication	Helicobacter Pylori	Gastric epithelial cells	Hypotonic lysis, mechanical disruption	Sonication	Clarithromycin	Delivered antibiotics to H. pylori bacteria by pathogen-host adhesion property	Angsantikul et al. (2018)
		RBC	Low-osmotic hemolysis	Ultrasound	Tedizolid phosphate	Advanced exotoxins neutralization; immune escape; anti-MRSA infection	Wu et al. (2021)
SARS-CoV-2	Malaria	CRL-2503, THP-1 cells	Hypotonic lysis, mechanical disruption	Sonication	/	Neutralized authentic SARS-CoV-2 in a dose-dependent manner <i>in vitro</i> ; without acute toxicity	Zhang et al. (2020a)
		THP-1 cells; RAW264.7	Hypotonic lysis, mechanical disruption	Sonication	Lopinavir	Alleviated the progression of CSS with reduced cytokines and NETs; carried drugs to the viral	Tan et al. (2021)
Others	Organophosphate poisoning	RBC	Hypotonic lysis, sonication and extrusion	extrusion	Dihydroartemisinin	Plasmodium infected RBCs targeting; a higher inhibition ratio and substantially lower ED 90	Zuo et al. (2022)
		RBC	Hypotonic lysis, sonication	Sonication	/	Reactivated AChE activity <i>in vivo</i> ; 100% survival rate of poisoned rabbits	Altaf et al. (2021)
Alzheimer's disease	Cardiac regeneration	T807-modified RBCM	Hypotonic lysis, extrusion	Sonication	Cur	Penetrated the BBB; targeting delivery Cur to neuronal p-tau	Gao et al. (2020b)
		Human cardiac stem cells	Three freeze-thaw cycles	Sonication	Stem cell factors	Acted as 'synthetic stem cells'; recapitulated stem cell functions in cardiac tissue repair	Tang et al. (2017)
CNV	Hindlimb ischemia	REC-RBC Hybrid	Hypotonic lysis + sonication	Sonication	/	Homotypic target and competitively bind to the VEGF	Li et al. (2021b)
		CXCR4-adipose-derived SCs	Hypotonic lysis + homogenize	Sonication	VEGF	Superior accumulation in ischemic tissue; rapid blood perfusion and limb salvage	Bose et al. (2018)
Image	FL	PEGylated MCF-7/CCM	Hypotonic lysis ultrasonics disruption	Extrusion	ICG	Homologous-targeting for FL/PA imaging; imaging-guided PTT	Chen et al. (2016)
		MDA-MB-831 cells	/	Microfluidic sonication	Imaging agents	Lower nonspecific uptake and enhanced tumor targeting	Liu et al. (2019)
US/PA	Platelet	Platelet	Hypotonic lysis	Extrusion	IR 780-1/ DOX	Higher penetration and retention in the brain for NIR imaging than PEGylated NPs	Kumar et al. (2019)
		Platelet	Repeated freeze-thaw	Sonication	Perfluoropropane	Detected early myocardial ischemia-reperfusion injury by US imaging in real time	Xu et al. (2021)
MRI	Neutrophil	Platelet	Repeated freeze-thaw	Sonication	Nanocarbon DOX, PFP	Phagocytosis escape; tumor target; PA/ US/ FL multimodal imaging; PTT/chemo therapy	Li et al. (2021a)
		Platelet	Repeated freeze-thaw	Sonication	Gadolinium	Detected well-developed atherosclerotic plaque and subclinical regions of arteries	Wei et al. (2018)
	A5-49 cells	Neutrophil	Hypotonic lysis and physical homogenization	Sonication	Superparamagnetic iron oxide	Diagnosed stroke-induced neuroinflammation with high sensitivity	Tang et al. (2021)
		A5-49 cells	Hypotonic lysis	Extrusion	Perfluorocarbons, ICG	Intravital ¹⁹ F MR/FL/PA tri-modal imaging-guided PTT	Li et al. (2020)

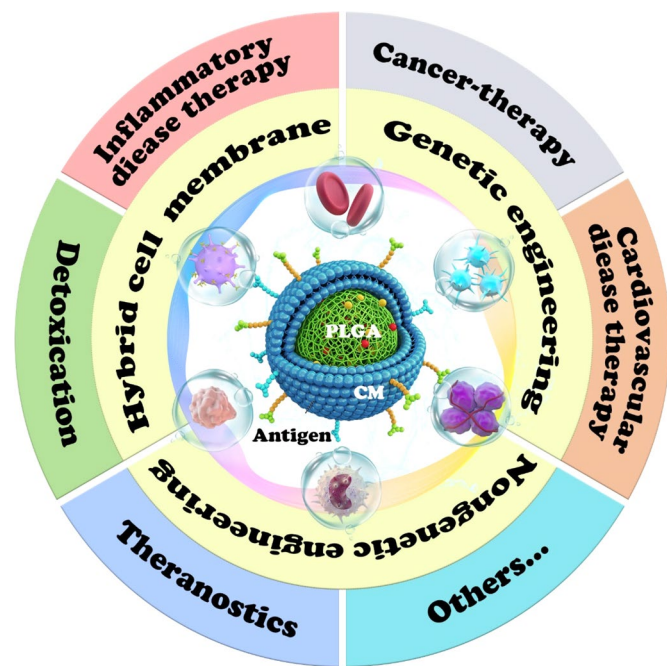


Figure 1 Schematic illustration of CM@PLGA biomimetic system for diverse biomedical application.

antimicrobial defense (Semple et al., 2011; Kunde & Wairkar, 2021). A variety of platelet-inspired therapeutic modalities, including platelet-rich plasma, platelet lysate, and platelet membrane (PM)-disguised bionic carrier, have been developed by utilizing the pathophysiological characteristics of platelets (Kola et al., 2021). Among these, PM-derived bionic carriers have attracted much interest because the inherent immune tolerance and long circulation (Hu et al., 2015). Similar to RBCM, PM is easy to extract, but PM show potential superiority over RBCM. The various platelet receptor families residing in PM phospholipid bilayer are accountable for high affinity toward various disorders like tumor, injured blood vessels, or inflamed area, which is essential for target drug delivery or diagnostics purpose (Kunde & Wairkar, 2021). PM disguised-PLGA bionic carriers also pretend to be decoys for detoxification and show great potential for treating immunopathy, such as immune thrombocytopenic purpura (Wei et al., 2016).

2.2. Eukaryotes

The cancer cell membrane (CCM) possesses some specific proteins, including Thomsen–Friedenreich antigen, galectins, and E-cadherin, which participate in cancer progression and metastasis through actively targeting homologous tumors via homotypic aggregation (Kondo et al., 1998; Glinisky et al., 2000). By virtue of merits that tumor cells are easy to proliferate *in vitro*, abundant CCMs such as 4T1, HepG2, and B16-OVA (B16 cells transfected with OVA antigen) can be obtained and employed as bionic carrier coats (Gou et al., 2021). Due to their superior homologous tumor homing, CCM allows targeted delivery for therapeutics or diagnostic reagents via Trojan horse approach. Further, the platform is

rich in cancer-specific antigens and can be used for vaccine development (Xiao et al., 2021).

Mesenchymal stem cell (MSC), a multipotent fibro-like cell isolated from skeleton, fat, embryos, and so forth, has been a potential candidate for regenerative medicine since its identification in 1987 (Hu et al., 2010). MSC is easy to be amplified *in vitro* and has been proven to be adept at immune surveillance evasion, inflammatory and lesion site migration (Nakki et al., 2017). Surface molecules, such as selectins, C-X-C chemokine receptor type 4 (CXCR4), integrin VLA-4, and proteases, are implicated in homing to the injured site, rolling and adhesion to endothelial cells (ECs), and transendothelial migration (Nitzsche et al., 2017). The functionalization of MSC membranes onto synthetic NPs not only retains the merits of low immunogenicity and inherent tumor tropism, but also has more advantages over living cells, such as ease of storage, higher drug loading and lower tumorigenesis (Wu et al., 2019a). They have present excellent performance in gene and drug delivery for a variety of cancer. For instance, human umbilical cord-derived MSC membrane-coated PLGA NPs exhibited enhanced liver tumor targeting (Yang et al., 2018). Further, the bionic platform also shows great therapeutic potential in myocardial infarction and osteogenesis due to the multifunction of stem cells (Luo et al., 2017; Liang et al., 2022).

Leukocytes or white blood cells are the largest blood cells and guard the body against disease. Once any pathogen invasion occurs, leukocytes timely respond and render amoeboid movements for passing through blood vessels to fulfill their duties (Oroojalian et al., 2021). Macrophages, T and B cells, natural killer cells, and dendritic cells (DCs) are all types of leukocytes, and each has its biofunction. For instance, neutrophils are among the innate immunity contributors to eradicate foreign invaders. Monocytes activated by pathogens become macrophages to protect the body from infection via phagocytosis and production of multiple inflammatory mediators. DCs exhibit antigen-presenting activity and activate antigen-specific T cells. Furthermore, they are implicated in the progression of some disorders, such as cancer and allergic diseases. Leukocyte membrane coating confers NPs with extended half-life, specific targeting, and passing through a biological barrier feature. Interestingly, a study has reported that macrophage membrane (MM) carriers work moderately better than living cells in atherosclerosis (AS) treatment (Gao et al., 2020a). Moreover, studies reported that nanoplateforms coated with polarized M1 macrophage membrane have better tumor-targeting capacity than that coated with unpolarized MM (Hu et al., 2020; Liu et al., 2020b). Nonetheless, some unpredictable biological effects and immunogenicity issues caused by the major histocompatibility complex of the membrane need further investigation (Oroojalian et al., 2021).

Apart from the popular choices of the above-discussed CMs, other relevant options have also been explored, such as ECs, beta cells, T cells, and activated fibroblasts (Fang et al., 2018; Dash et al., 2020). Each cell possesses a particular advantage as well as an inherent defect. Abundant anucleate cells, either drawn from the blood of patients or donated blood, are needed. These sampling procedures

incurs high-cost and plague will impede access to donated blood. Eukaryotic cells are easy to be amplified, but the extraction process is relatively complex. Hence, the choice of PLGA preparations with different CM camouflages should be based on the disease type and patient affordability.

Regarding the construction of CM@PLGA NPs, membrane isolation techniques, coating processes, and characterization approaches have been discussed in detail in Oroojalian's review (Oroojalian et al., 2021). Briefly, cells are first disrupted by hypotonicity, sonication, or repeated freeze-thaw cycles to obtain CM vesicles, which is followed by coextrusion or sonication with PLGA NPs to obtain biomimetic core-shell NPs. Extrusion is simple but not conducive to mass production. Ultrasound (US) provides a high yield, but the local high temperature may damage the protein structure. Recently, novel microfluidic technology has been investigated for possible high-volume production.

The CM vesicles and PLGA contact may be favored by hydrophobic interaction in order to reduce the free energy of the system (Bose et al., 2016). The electrostatic repulsion between negatively charged PLGA and asymmetrically charged CM results in a right-side-out membrane orientation on CM@PLGA NPs (Luk et al., 2014). This orientation has been confirmed via the localization of CD47, CD44, and CXCR4 proteins, and the quantification of glycoprotein content and sialyl groups on the membrane surface (Luk et al., 2014; Jin et al., 2019). Moreover, the PLGA polymer branch is inserted into the phospholipid layer, thus, forming a hydrophobic force and hydrogen bonding with the phospholipid layer. Therefore, the stability of CM@PLGA nanosystem is stronger than that of CM-wrapped mesoporous silicon NPs or CM-inorganic hybrid nanoplateforms. The high stability of CM@PLGA reduces the leakage of the drug and prolongs its circulation time in the body.

3. Strategies for engineering CM-derived vesicles

For optimal therapeutic management, researchers are excited to design smart nanoplateforms by functionalizing CM vesicles to improve tissue penetration and targeting capacity, thus, reducing off-target effects (Table 2). For instance, RBC lacks specific proteins responsible for active targeting; therefore, functional ligands attached to the RBCM can widen its applications. Genetic engineering, chemical conjugation, and lipid insertion method can be applied to introduce various functional groups into CM-derived vesicles (Li et al., 2022). Furthermore, new hybrid membranes with the desired multitasking ability can be obtained by the direct fusion of CMs from different sources (Liu et al., 2021).

3.1. Genetic engineering

Genetic engineering is a versatile premodification technique to produce additional membrane proteins before the disruption of the parent cells. Human adipose-derived stem cells (SCs) harboring CXCR4 were bioengineered using a retroviral vector system (Bose et al., 2018). Owing to the interaction

between CXCR4 embedded in the membrane and stromal cell-derived factor-1 (SDF-1) secreted by the injured tissues, the targeting capability, and retention time in ischemic hind-limb were robustly improved for over 14 days after the intravenous administration, whereas the nonengineered vesicles lasted only 3 days. By utilizing the CXCR4/SDF-1 axis, MSCs mimicking PLGA NPs were accumulated in the bone, and the sustained release of paracrine molecules facilitated osteoporosis treatment (Zhang et al., 2022a). T cell receptor engineered T cell therapy (TCR-T) is one of the great democratizing stories of recent years. TCRs capable of recognizing certain tumor antigens were genetically engineered into T cells derived from the patient's peripheral blood (Morgan et al., 2006). CM derived from T-cell hybridoma endowed with a melanoma-specific anti-gp100 TCR was used to disguise the PLGA NPs (Yaman et al., 2020). The presence of anti-gp100 TCR led to a threefold increase in cellular uptake and a more than twofold increase in tumor retention compared with the control group.

Recently, tumor necrosis factor-related apoptosis-inducing ligand (TRAIL) genetically expressed-human umbilical vein EC (HUVEC) membrane tremendously increased the effective concentrations of oxaliplatin and hydroxychloroquine (autophagy inhibitor) encapsulated in PLGA by 21 and 13 times, respectively, at the tumor site compared with the free-drug mixture (Shi et al., 2021). Because of the existence of chemotherapeutics-triggered protective autophagy in patients, the study embodied good clinical foresight. To target Clec9a⁺ DCs, engineered peptide CBP-12-expressing CCM-coated nanovaccine (named PLGA/STING@EPBM) was developed with co-delivered tumor antigen and interferon stimulating gene agonist 2'3'-cGAMP (Figure 2(a)). A retroviral vector was designed to encode His-tagged CBP-12, which was successfully expressed on CM (Figure 2(b-d)). The core-shell structure of nanovaccine was clearly visible (Figure 2(e)). CBP-12 modification favored antigen uptake and reduced the 2'3'-cGAMP dosage by approximately sixfold to 238-fold (Gou et al., 2021). Dose reduction facilitates fewer side effects, lower medication costs, and improved accessibility.

In addition to the use of viruses as transgenic vectors, Lipofectamine 3000 is also available for transducing specific membrane proteins (Li et al., 2021c). Genetic engineering stably expresses specific proteins on the CM, thereby avoiding alterations in the original biological function of the CM as a result of chemical operations. Nevertheless, gene editing *in vitro* is impossible for anucleate cells. Moreover, gene transfection efficiency has been the primary domain of research, and nonviral systems are usually limited by their inefficiency. In future studies, the quantity and homogeneity of specific proteins on the surfaces of vesicles should be identified and tailor-made for specific applications.

3.2. Nongenetic engineering

Nongenetic engineering is also a robust and versatile approach to anchoring functional molecules on cell surfaces and is particularly suitable for akaryotes or functional groups that cannot be produced via genetic engineering. Chemical modification

Table 2. Engineering strategies of CM-derived vesicles.

Engineering method	Modification groups	CM source	Membrane extraction	Cargos	Disease	Ref	
Genetic engineering	CBP-12	B16-OVA, TC1, 4T1	Membrane protein extraction kit	STING agonist 2'3'-cGAMP	Melanoma; lung cancer; metastatic breast cancer	Gou et al. (2021)	
	CD47; integrin $\alpha 4\beta 1$	RAW 264.7	Hypotonic lysis	Colchicine	AS	Li et al. (2022)	
	CXCR4	Human adipose-derived SC	Hypotonic lysis + homogenize	VEGF	Hindlimb ischemia	Bose et al. (2018)	
	Anti-gp100 T-cell receptor	T cells 19LF6	Hypotonic lysis	Trametinib	Melanoma	Yaman et al. (2020)	
	TRAIL	HUVEC	Lysis	Oxaliplatin + hydroxychloroquine	Hepatoma	Shi et al. (2021)	
	TLR4	RAW264.7	Freeze-thaw cycles	Tasquinimod	UC	Li et al., (2021c)	
	M2pep	KPC	Hypotonic lysis + freeze-thaw cycles	Gemcitabine	Pancreatic cancer	Wang et al. (2022a)	
	CXCR4	NSC	Hypotonic lysis + freeze-thaw cycles	Glyburide	Stoke	Ma et al. (2019)	
	TRAIL	HUVEC	Hypotonic lysis + sonication	Hydroxychloroquine	RA	Shi et al. (2020)	
	Chemical conjunction	Recombinant hyaluronidase	RBC	Hypotonic lysis + extrusion	/	Prostate cancer	Zhou et al. (2016)
Lipid insertion		Anti-EGFR-iRGD	RBC	Low osmotic pressure	Gambogic acid	Colorectal cancer	Zhang et al. (2018b)
		Galactose T7 peptide	RBC	Hypotonic lysis	Baicalin + Hgp100 ₂₅₋₃₃ + CpG	Melanoma	Han et al. 2019)
		¹⁸ WSW and NGR peptide	RAW 264.7	Hypotonic lysis + extrusion	Saikosaponin D	Breast cancer	Sun et al. (2020a)
Hybrid CM	T807	RBC	Hypotonic lysis + extrusion	Euphorbia factor L1	Glioma	Cui et al. (2020)	
	Folic acid	RBC	Hypotonic lysis	DOX and ICG	Alzheimer's disease	Gao et al. (2020b)	
	DC-MC38 or DC-GL261		Hypotonic lysis + freeze-thaw cycles	CpG	Hepatoma	Chen et al. (2021)	
	DC-ID8		Hypotonic lysis + freeze-thaw cycles	CpG	Colon carcinoma; glioma	Ma et al. (2020)	
	RBC-platelet		Freeze-thaw cycles	/	Ovarian cancer	Zhang et al. (2022b)	
	143B-RAW264.7		Isolation buffer + ultrasound	PTX	Detoxification; metastatic cancer; AS	Dehaini et al. (2017)	
	RAW264.7-4T1		Freeze-thaw cycles	DOX	Osteosarcoma	Cai et al. (2022)	
RBC-REC		Hypotonic lysis; homogenization and sonication	/	Metastatic breast cancer	Gong et al. (2020)		
					CNV	Li et al. (2021b)	

and physical lipid insertion are the two main strategies, and each one has its pros and cons (Wang et al., 2015).

3.2.1. Chemical modification

Chemical modification refers to the formation of covalent bonds between the reactive primary amines on the CM and the activated carboxylic acid, which enables the stable anchorage of functional molecules (Wang et al., 2015). To improve the penetration of the nanocarrier into the tumor tissues, Zhou et al covalently modified recombinant hyaluronidase (rHuPH20) with the amino group of living RBC in a two-step process via a cell-impermeable linker NHS-PEG-Maleimide with different linker molecule lengths (Zhou et al., 2016). The natural function of the RBCM was not compromised. PH20-RBCM-NPs enhanced NPs diffusion through

extracellular matrix-mimicking gels and degraded the pericellular hyaluronic acid matrix of the PC3 cells. Interestingly, the long linker (MW: 3400) was more conducive to sustaining the enzyme activity than its short counterpart (MW: 425). The advantages of chemical grafting are that the density and length of the modified molecules are controllable, and the stable anchoring is particularly appropriate for biological macromolecules. However, the linkers must be carefully chosen to ensure that the conformation of the modified molecule or the biological function of the CM is not altered during the chemical reaction.

3.2.2. Lipid insertion method

Lipid insertion method relies on the physical insertion of a ligand into the lipid bilayers with the aid of hydrophobic lipid tethers, which can maintain the biological activity of the functional

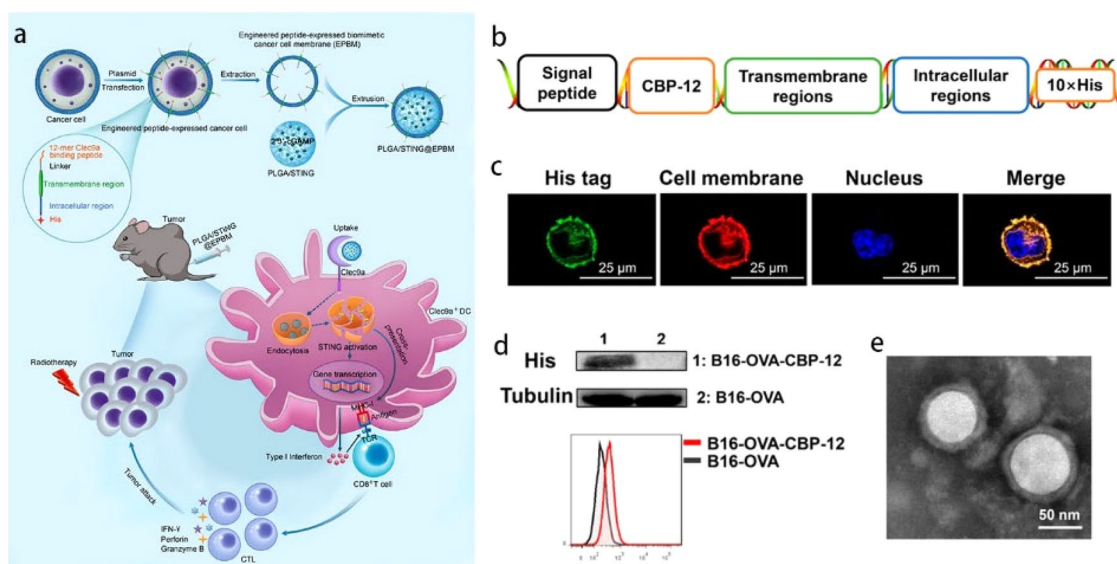


Figure 2. (a) PLGA/STING@EPBM structure and strategy for enhancing antitumor immunity. (b) A retroviral vector encoding His-tagged CBP-12 to transfect B16-OVA cells. (c) Confocal laser scanning microscope images, (d) Western blot and flow cytometry confirmed CBP-12 successfully expressed on CM. (e) TEM of PLGA/STING@EPBM (Gou et al., 2021). Copyright 2021 American Chemical Society.

molecules and the intact structure of membrane protein to the best possible extent. In a study, N-succinimidyl palmitate was used to lipidate anti-EGFR-iRGD recombinant proteins, and then, insert them into RBCM, followed by enveloping PLGA NPs. Owing to the tumor penetrating iRGD peptide and EGFR targetability, the designed nanoplatforms were able to deeply penetrate the multicellular spheroids *in vitro* and accumulate efficiently in colon cancer with high EGFR expression *in vivo* (Zhang et al., 2018b). Another study exploited galactose-decorated RBCM-coated PLGA NPs for reversing tumor-associated macrophages (TAMs) with overexpressed galactose-type lectin. DSPE-PEG-Gala was incubated with RBCM for 30 min (Han et al., 2019). Alternatively, MM was hybridized with DSPE-PEG-T7 peptide to leverage MM-homing and tumor-recognizing capacity to overcome distal metastasis (Sun et al., 2020a).

The blood-brain barrier (BBB) has always been a problem in the treatment of brain diseases. Dual-targeting ^DWSW and NGR peptide-decorated RBCM were applied to penetrate the BBB and blood-brain tumor barrier, respectively (Cui et al., 2020). Lipid tether DSPE-PEG₂₀₀₀-^DWSW and DSPE-PEG₂₀₀₀-NGR were synthesized using the sulfhydryl-maleimide coupling method and then incubated with RBCM at 37°C for approximately 0.5 h. After loading the euphorbia factor L1 in the PLGA NPs, these nanomedicines were able to target the C6 glioma cells and the cytotoxicity rate was twofold higher than that of the unmodified NPs in the BBB/C6 coculture model. In another study, T807, a novel neuron tau PET imaging agent, was attached to the RBCM (Figure 3(a)). The linker DSPE-PEG3400-T807 was obtained by coupling the amino-T807 with DSPE-PEG3400-NHS (Figure 3(b)). The core-shell structure NPs could effectively cross the BBB and target tau within the neurons in Alzheimer's disease (Figure 3(c-f)). The concentration of Cur-loaded bionic NPs in the brain was 6.3 times higher than that of free Cur (Gao et al., 2020b).

In addition to small-molecule ligands and protein polypeptides, other diverse modified materials are available.

Cholesterol-modified AS1411 aptamers can be tethered to biomimetic NPs for targeting nucleolin on tumor cells (Han et al., 2020). The ligand-linker-lipid insertion approach based on hydrophobic interaction is simple and mild and avoids the use of strong organic reagents or exhaustive purification steps. However, one concern is that the linking of the protein to the lipid tail needs to be carefully performed to minimize alterations in protein conformation. Another concern is the need for an accurate quantification method to determine the proportion of modification on the membrane surface.

3.3. Hybrid cell membranes

Hybrid CM, which is modified with different types of CM is yet another strategy to equip the CM vesicles with multiple intrinsic biofunctions inherited from the original parent cells (Chen et al., 2020a). The erythrocyte-platelet hybrid membrane, which retains the characteristic membrane protein of each cell and combines the detoxification ability from erythrocytes with specific adhesion to metastatic cancer cells or AS from platelets, is the opening example by Dehaini et al. (Dehaini et al., 2017). There are several hybrid membranes of different cell types that wrap PLGA core thus far, such as platelet-neutrophil (Ye et al., 2020), erythrocyte-cancer cell (Wang et al., 2020), osteosarcoma cell-macrophage (Cai et al., 2022), and human monocyte-genetically engineered cell hybrid membrane (Rao et al., 2020). In addition to the natural CM fusion, the hybridization of CM-synthetic materials such as liposomes is also available (Wu et al., 2020).

Hybrid membranes were prepared not only by fusing live cells preceding the membrane extraction but also by fusing the CM nanovesicles. In order to resolve the unsatisfactory clinical trial outcomes of DC-based immunotherapy, DC-tumor fusion CM@PLGA NPs were fabricated to co-present whole tumor antigens and costimulatory molecules (Figure 4(a)) (Ma et al., 2020). Briefly, DCs activated by lipopolysaccharide

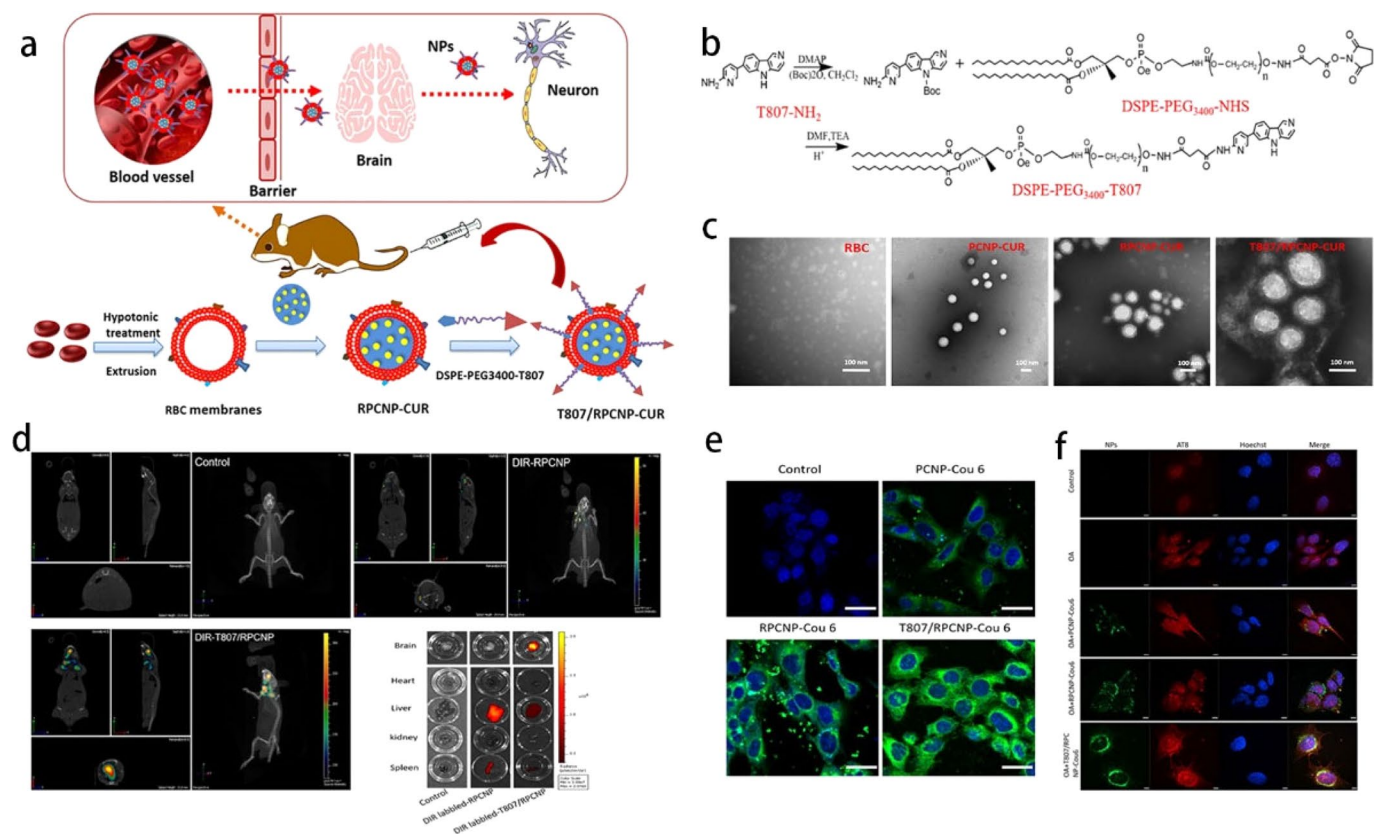


Figure 3. (a) Schematic illustration of T807/RPCNP-CUR accumulation in neurons. (b) The preparation of DSPE-PEG3400-T807. (c) TEM of various NPs. (d) *In vivo* brain-targeting ability. (e) HT22 neuron cells and (f) p-tau (red fluorescence) targeting capability (Gao et al., 2020b). Copyright 2020 Springer Nature.

(LPS) were fused with MC38 or GL261 cells in the presence of PEG (MW 1500Da) (Figure 4(b)), followed by hypotonic lysis and freeze-thaw process to extract the CM of the fusion cells. Unlike the fusion cells, NPs of smaller size (100 nm) penetrated the lymphoid organs more easily to evoke T-cell activation (Figure 4(c,d)). Furthermore, DC-GL261 fusion CM@PLGA NPs can cross the BBB and inhibit glioma development. As supported by a latest report, the fusion CM nanovaccine showed strong selectivity for cognate tumor in different patient autologous ovarian cancer xenograft models (Zhang et al., 2022b). Conversely, MM and CCM vesicles were first derived from RAW264.7 and 4T1 cells and then fused for metastatic cancer treatment (Figure 4(e)) (Gong et al., 2020). The hybrid membrane fusion was confirmed by the Förster resonance energy transfer (FRET) method. Specific biomarkers of each cell were then verified by Western blot and immunogold-labeling of TEM (Figure 4(f-h)). Owing to the homotypic homing and $\alpha 4$ integrin-VCAM-1 (vascular cell adhesion molecule-1) interaction, DiR-PLGA@[RAW-4T1] NPs accumulation approached 5.14-fold greater in lung metastasis and 20-fold lower in the liver relative to those of uncoated NPs. Importantly, lower DOX leakage benefit from the CM coat in the physiological environment also reduced the relevant side-effects (Figure 4(i)).

Hybrid membrane fusion-disguised PLGA NPs, instead of a mixture of single membrane-coated NPs, recapitulated the functions of source cells and exhibited much better behavior than their counterpart. Researchers have been inspired to

customize different hybrid membrane groups according to the diverse disease pathology. Careful consideration is, however, warranted on the optimized productive membrane fusion method and the relative quantities of each source CMs. These technologies can possibly enrich the functions of CM@PLGA to achieve therapeutic purposes. The construction of engineered CM-camouflaged nanovesicles is the current trend in this particular research field.

4. Application of CM@PLGA nanoplatfoms

4.1. Cancer therapy

4.1.1. Chemotherapy

CM@PLGA offers unique advantages in delivering antitumor drugs. On one hand, PLGA can be loaded with different types of therapeutic drugs (such as hydrophilic drugs, hydrophobic drugs, and proteins) and exhibit a sustained-release effect. On the other hand, the encapsulation of CM can overcome the drug leakage of PLGA, protect drugs from enzymatic hydrolysis, and target drug delivery. For example, RBCM significantly increased the area under curve, half-life, and the relative bioavailability of obatoclax mesylate-loaded PLGA NPs by 8.8-, 2.5-, and 4.0-times when compared with free obatoclax mesylate, respectively, which facilitate further drug accumulation in the tumor tissues (Chen et al., 2020b). The combination of RBCM and PLGA promotes stability and biocompatibility *in vivo* and also

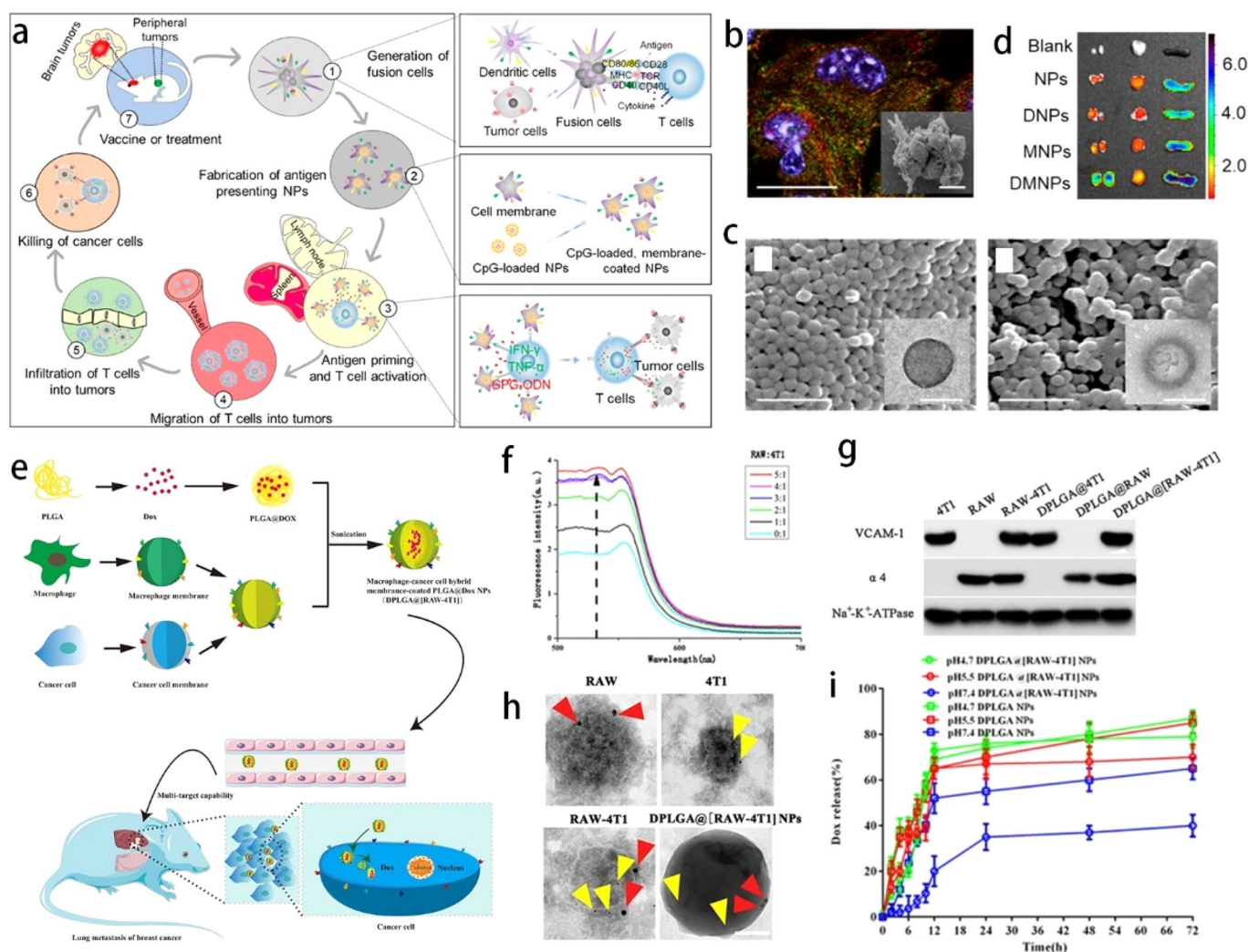


Figure 4. (a) Synthesis and utilization of whole tumor antigen presenting costimulatory NPs. (b) Representative images of DC-MC38 fusion cells. (c) PLGA and hybrid CM-coated NPs captured by SEM (scale bar: 500 nm) and TEM (insert, scale bar: 50 nm). (d) The accumulation of the indicated NPs in the lymph nodes, thymus, and spleen after intravenous administration (Ma et al., 2020). Copyright 2020 American Chemical Society. (e) Formation and multitargeting of DPLGA@[RAW-4T1] NPs to lung metastatic. (f) FRET, (g) Western blot, and (h) immunogold TEM images confirmed the membrane fusion. (i) DOX release behavior (Gong et al., 2020). Copyright 2020 Springer Nature.

broaden clinical applications of other potential antitumor drugs. Some defects such as the irritating blood vessels or allergic reactions of the conventional cosolvents ethanol or Tween can be exempted (Zhang et al., 2017).

The PLGA core can be devised to encapsulate multiple drugs with different action mechanisms for enhanced therapeutic efficacy (Jiang et al., 2018). For instance, vitamin E TPGS was used to prepare RBCM-cloaked porous PLGA. The resultant porous structure and enhanced surface area may have elevated drug encapsulation (>93.8%). The RBCM acted as a diffusional barrier to suppress burst drug release of PLGA NPs in the first 12 h (Xie et al., 2019). DOX and icotinib (EGFR tyrosine kinase inhibitors) co-loading PLGA coated by H1975 CMs demonstrated superior homologous targeting ability and overcame drug resistance in EGFR-mutated lung cancer. After coating with the CM, the DOX leakage of PLGA NPs was found to be reduced from 40% to 30% within 48 h at pH 7.4 (Wu et al., 2019b). Recently, TE10 CCM and DSPE-PEG were self-assembled on PLGA NPs dual-loading with DOX and a chemotherapeutic sensitizer Cur to overcome the multidrug resistance of esophageal carcinoma (Gao et al., 2021). As

displayed in Table 1, CM@PLGA has been most widely studied for chemotherapeutic drug delivery.

4.1.2. Gene therapy

Chemo-gene combined therapy has been a promising cancer treatment modality. In past research, HeLa CM-wrapped PLGA NPs were developed for PTX and E7-targeting siRNA co-delivery (Xu et al., 2020). CCM coating overcame the defect of immune clearance of PLGA and the 'self-homing ability' endowed tumor sites with the preferential accumulation as threefold higher than that of bare NPs. Carcinogenic genes E7 knockdown increased the intracellular PTX concentration by inhibiting the AKT pathway activation and the expression of the multidrug resistance protein, which resulted in an 83.6% of tumor inhibition rate. Furthermore, the hematological toxicity of PTX was alleviated and no pathological changes were noted in the liver. However, this biomimetic platform for gene transfer has rarely been reported, possibly due to the poor gene-loading efficiency resulting from the hydrophobicity and electronegativity of PLGA. Contrary to

Zhang's theory stating that negatively charged cores favor the right-side-out membrane orientation and proper formulation of bionic NPs (Luk et al., 2014), increasing numbers of the cationic cores-based bionic system have been reported (Hao et al., 2018; Wang et al., 2019a). Conversely, the interface interaction between the cationic core and CM warrants further elucidation. Nevertheless, by modifying PLGA with cationic substances or chemical conjugation as in our previous study (Zheng et al., 2022), followed by CM camouflage, the dilemma of low gene encapsulation efficiency and targeted delivery can be resolved. The combination with US technology can mediate endosome escape by forming holes, which is essential for gene release and high-transfection efficiency (Mura et al., 2013). Presently, this biomimetic nanotechnology has revolutionized the development of drug delivery platforms in onco-therapeutics.

4.1.3. Immunotherapy

Cancer immunotherapy, such as chimeric antigen receptor-T cell therapy, immune checkpoint blockade therapy, and neo-antigen vaccines has achieved remarkable clinical efficacy during the past decade (Mi et al., 2019). Recently, scientists

have dedicatedly explored different immunotherapy strategies to overcome the immunosuppressive tumor microenvironment (TME) and stimulate the relevant immune responses to defeat cancer. For instance, T-cell-derived PLGA NPs, an imitator of cytotoxic T-lymphocytes (CTLs), have been reported to reverse TME by preventing CTLs depletion and immune-checkpoint blockade in an antigen-nonspecific manner (Kang et al., 2020). Tumor immunogenic cell death (ICD), induced by chemotherapy, phototherapy, or other mechanisms, unleashes tumor-associated antigens (TAAs) to stimulate immunity (Lesterhuis et al., 2011). However, the TME overshadows the number and functions of immune cells. A combination of DOX-loaded NPs coated by RAW 264.7 CM with lymphotactin (XCL-1)-loaded sodium alginate was designed to work along both the lines (Figure 5(a)) (Xiong et al., 2021). DOX-loaded PLGA exhibited an ideal sustained drug release effect with 48.93% of DOX released within 72 h. Because of the blocking effect of CM, the drug release rate of CM@PLGA was reduced to 44.98% within 72h. MM facilitated DOX enrichment in the tumor (4.11-fold greater than that of DOX) and increased CRT and HMGB1 expression, indicating a more efficient ICD (Figure 5(b,c)). XCL-1 constantly released from *in situ* hydrogels specifically recruited XCR-1+

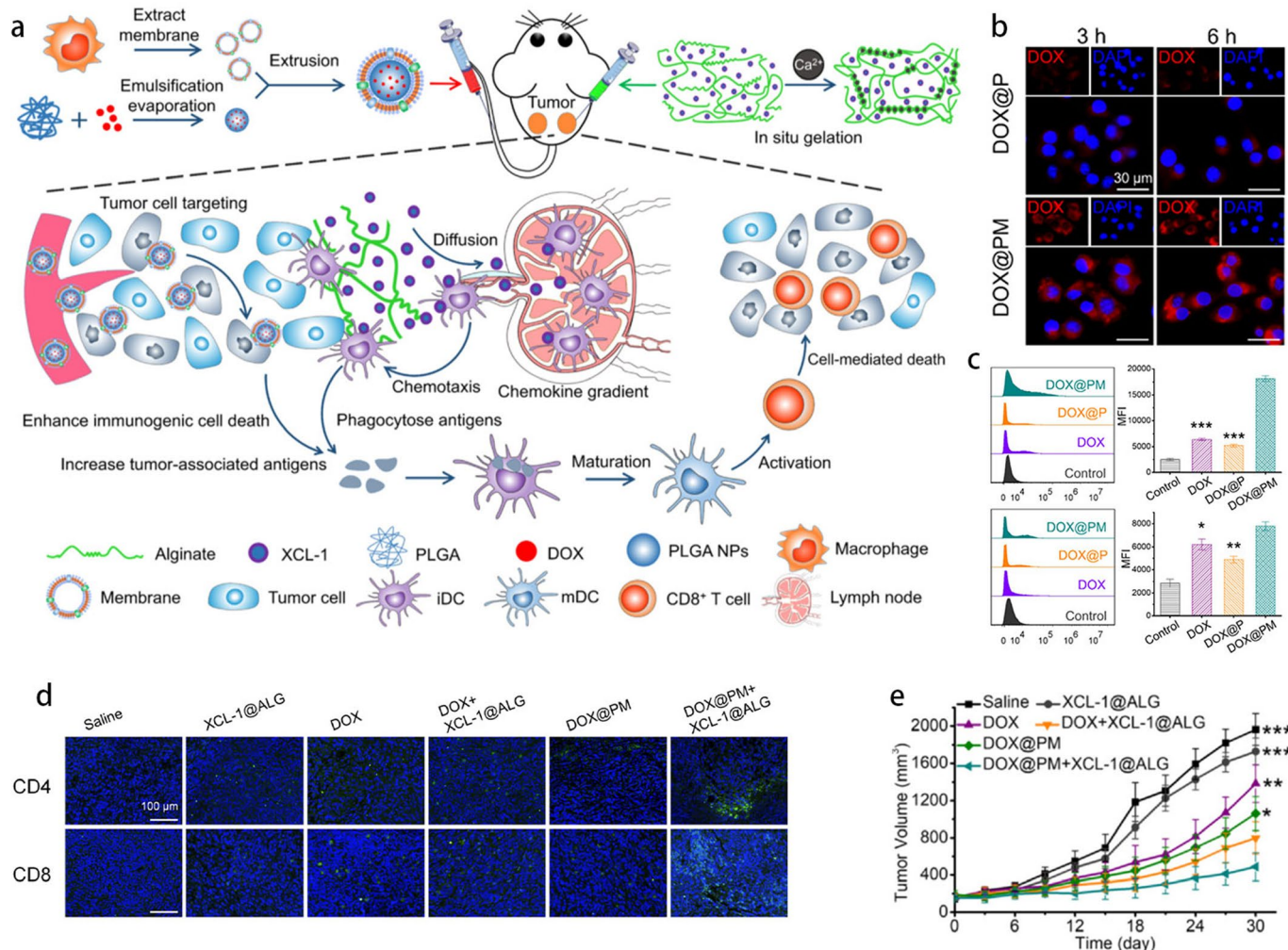


Figure 5. (a) Schematic illustration of DOX@PM, the gelation of XCL-1 loaded sodium alginate *in situ* and mechanisms of enhanced ICD and activated antigen cross-presentation. (b) *In vitro* tumor cells targeting. (c) Flow cytometry of CRT-positive and HMGB1-positive 4T1 cells. (d) Immunofluorescence staining of CD4⁺ and CD8⁺ T cells (green color) in tumor tissues. (e) Tumor volume at the right side in various formulations (Xiong et al., 2021). Copyright 2021 Elsevier.

DCs for capturing TAAs, and then, activated CD4⁺ and CD8⁺ T-cells to the homolateral tumor (Figure 5(d)). An excellent homolateral tumor inhibition rate (75.15%) in 4T1-tumor-bearing mice indicated the double enhancement of ICD and immunotherapy (Figure 5(e)).

Inspired by the unique tumor-targeting advantages, MM modified with cationic PEI further promoted antigen and immunopotentiator uptake and conspicuously boosted humoral and cellular immune responses (Zhang et al., 2020b). Alternatively, LPS-treated MM-coated NPs encapsulating Fe₃O₄ and imiquimod were employed for polarizing TAMs instead of targeting the tumor cells. The immunotherapy was potentiated by synergetic activated IRF5 and the NF-κB signaling pathway by Fe₃O₄ and imiquimod, respectively (Liu et al., 2020a). Recently, bioengineered CCM that overexpresses peptides targeting M2 macrophages guided the notion of 'one stone (gemcitabine) kill two birds (both cancer cells and TAMs)' (Wang et al., 2022a). Indeed, the CM-based bionic platform is high profile for enhanced antigen or adjuvant delivery as well as macrophage polarization in TME.

Given the ability to deliver TAAs, the CCM-based biomimetic platform occupies a valuable niche in vaccine development (Jin et al., 2019). This system can help develop promising individualized vaccines with the increment in CTLs and IFN γ in the immunized mice. Breast cancer metastasis was inhibited as a result of the disturbance of the stromal-cancer cell interaction for the first time. However, the author argued that the appearance of CCM antigen, rather than PLGA NPs, may accelerate the clearance rate (Jin et al., 2019), which conflicts with a past report (Xu et al., 2020). Another novel study clarified the immune memory establishment mechanism of the nanovaccines possessing the antigenic shell of CCM (Xiao et al., 2021). These nanovaccines boosted the DC maturation, which subsequently secreted cytokines to suppress Treg differentiation from CD4⁺ T-cells and promoted CD8⁺ T-cells to differentiate into central-memory (T_{CM}) and effector-memory (T_{EM}) T-cells. When the BALB/c mice were vaccinated thrice and challenged with 4T1 cells, T_{CM} and T_{EM} of the pre-trained immune system could differentiate into CTLs to recognize and eliminate the cancer cells. The potentiating immunotherapy could free the patients from chemotherapy drugs.

4.1.4. Phototherapy

Owing to negligible invasiveness, high selectivity, ease of remote spatiotemporal control, light radiation of a specific wavelength has been employed in phototherapy (Mura et al., 2013). Phototherapy, including photothermal therapy (PTT) and photodynamic therapy (PDT), not only directly eliminate tumor by heat energy or reactive oxygen species (ROS) but also trigger the on-demand local release of chemotherapeutics. Importantly, phototherapy combined with biomimetic nanocarriers has emerged as a highly promising therapeutic strategy.

Despite the conspicuously improved payload delivery, the intact CM on the NP's surface may block the drug release at the tumor site. An FDA-approved photosensitizer indocyanine green (ICG) can absorb near-infrared (NIR) light with a wavelength of >750 nm and convert it into fluorescence, heat energy, and simultaneously produce ROS (primary PTT

and minor PDT) (Sun et al., 2021). NIR-triggered DOX and ICG co-loaded RBC mimetics leveraged excellent photothermal conversion performance of ICG. Upon 808-nm laser irradiation (1.5 W/cm²), the local temperature remarkably increased from 33 °C to 75 °C within 10 min *in vitro* and approximately 89.6% of DOX at pH 5.5 was released within 120 h (Chen et al., 2021). Recently, to overcome chemoresistance in breast cancer, an elaborate dual-target and multirelease smart DDS co-encapsulating DOX, Mcl-1-siRNA and photothermal iron-oxide NPs (ICG covalently attached to IO) in the PLGA-chitosan cores, was finally cloaked with MCF-7 CM (Figure 6(a)) (Guo et al., 2022). The greater and faster release profile of DOX (~83%) and Mcl-1-siRNA (~71%) was attributed to the high solubility of chitosan and increased hydrolysis of PLGA at pH 5.5 combined with laser irradiation (Figure 6(b,c)). Dox efflux from MCF-7/ADR cells was significantly suppressed due to Mcl-1 silence (Figure 6(d)). Conversely, MCF-7 homotypic affinity and magnetic targeting render NPs with considerable tumor enrichment (Figure 6(e)). The synergistic chemo-PTT generated an almost 80% inhibition rate in an MCF-7/ADR tumor model (Figure 6(f)), accompanied by an insusceptible influence on the heart and liver functions.

In the above studies, the main role of the CM was to block the PLGA tunnels and achieve tumor-targeting drug delivery. The following further study will demonstrate another important role of the CM shell. As a phospholipid bilayer, CM can load hydrophobic molecules to enhance the treating effect of chemotherapeutic drugs loaded in PLGA. In previous research, a PDT agent, chlorin e6 (Ce6), when inserted into RBCM, produced ROS under a mild 660-nm LED light (5 mW/cm², 10 min), causing membrane damage and rapid DOX or biological macromolecular drugs release (Gao et al., 2017a). Another recent study reported a structure-changeable NP with pyropheophorbide a-inserted RBCM. The photolytic removal of the coat and inner core exposure accelerated cellular uptake hindered by RBCM (Liu et al., 2022). Indeed, the PDT response is more sensitive than that of PTT as the latter required higher power density and irradiation time, which may cause permanent skin damage. Inspired by the above studies, CM@PLGA can be constructed as a dual drug-loaded nanosystem for multimodal tumor combined therapy, such as chemo-immune synergistic therapy and light-radiation synergistic therapy. This will further enrich the application of CM@PLGA in medical science. More interestingly, this dual drug-loading system possesses the sequential drug-releasing feature, in which molecules loaded in the CM gets released in a limited manner, followed by a slow release of the drug in the PLGA. Thus, CM@PLGA can be used for the treatment of some special diseases, such as psoriasis, wound healing, osteogenic differentiation, and anovulatory dysfunctional uterine bleeding.

4.1.5. Other anticancer strategies

Other strategies also present alluring potentials. In order to alleviate the hypoxic TME of most solid tumors and enhance the chemotherapy or radiotherapy efficacy, CCM-camouflaged PLGA nanovectors have been reported to transport

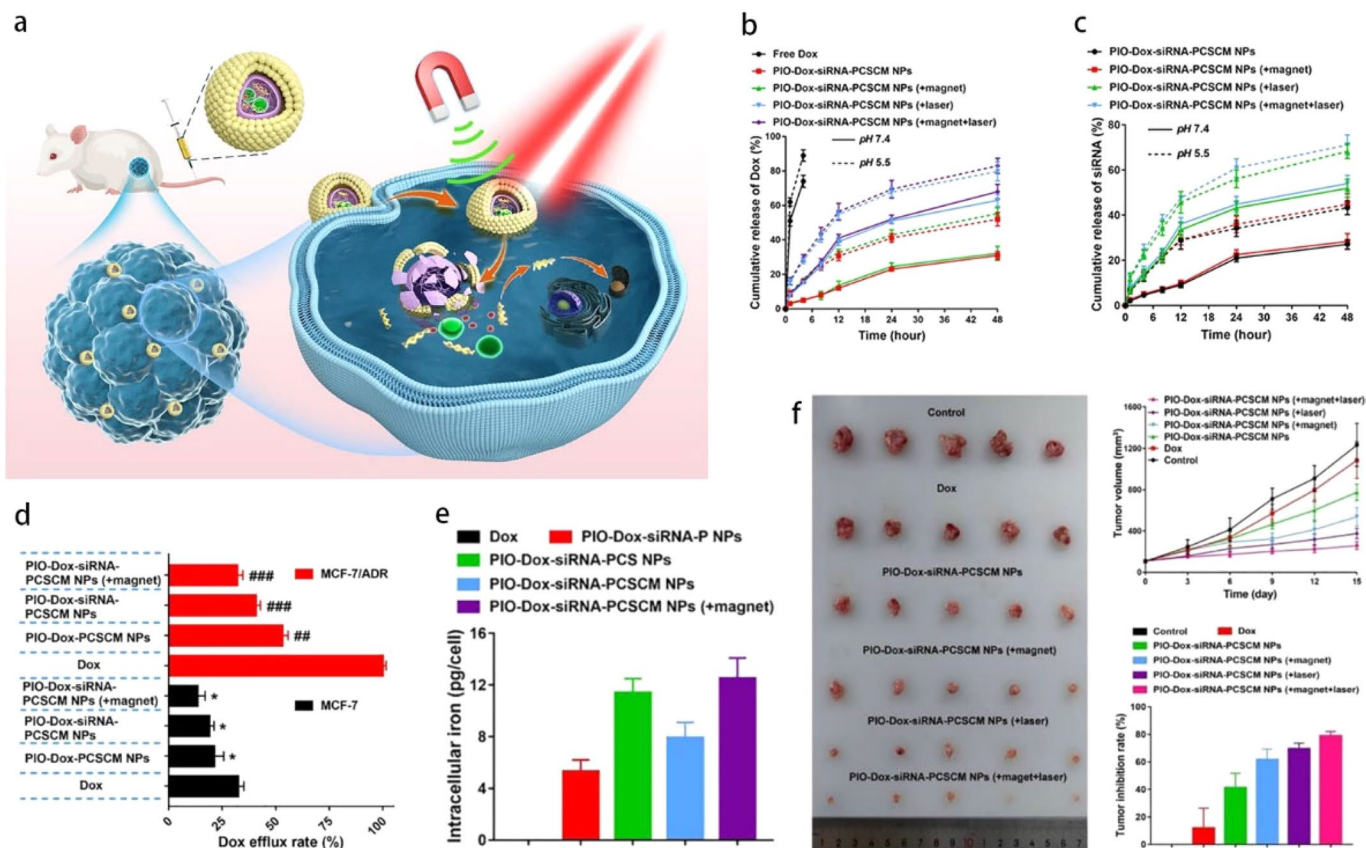


Figure 6. (a) Schematic illustration of magnetically targeting NPs. NIR irradiation triggered drug release to result in chemo-PTT of drug resistant breast cancer. Cumulative release of (b) Dox and (c) Mcl-1-siRNA. (d) Dox efflux rate and (e) intracellular iron content in MCF-7/ADR cells. (f) Tumor suppressive effect (Guo et al., 2022). Copyright 2022 Elsevier.

hemoglobin and DOX to the homologous tumor and break the hypoxia-induced chemoresistance by O_2 self-sufficiency (Tian et al., 2017). The CCM-camouflaged nanovectors exhibited promising oxygen-carrying capacity owing to the structure of PLGA core and the hemoglobin loaded in the PLGA. The CM shell could reduce the leakage of oxygen during circulation. As a result, the designed nanoplateforms achieved an excellent antitumor effect. In another study, an artificial perfluorocarbon-loaded RBC mimicry PLGA nanoplateforms can absorb oxygen within the pulmonary capillaries. The prolonged blood circulation and nanoscale are favorable for diffusion deep into solid tumors that significantly increase the oxygenation level from 1.6% to 24%; subsequently, radiotherapy efficiency is remarkably enhanced without notable additional side-effects on the major organs (Gao et al., 2017b). The aforementioned studies demonstrated that CM@PLGA is an excellent gas delivery vehicle due to the high gas-loading capacity of PLGA and the blocking effect of CM. In addition to oxygen, it is suggested that CM@PLGA can be used to deliver therapeutic gases (such as CO, NO, and H_2S) for cancer therapy in the future.

A biomimetic gas nanofactory loading glucose oxidase (GOx) and $Mn_2(CO)_{10}$ was designed in a combination of starvation therapy and gas therapy (Wang et al., 2019c). Briefly, GOx and $Mn_2(CO)_{10}$ were encapsulated into the PLGA and then coated by RBCM. Glucose is catalyzed by GOx to produce H_2O_2 . The concomitant production of H_2O_2 can effectively trigger CO release from $Mn_2(CO)_{10}$, which causes

mitochondrial dysfunction of the cancer cells. Meanwhile, glucose depletion leads to cutting off of its energy supply to starve the cancer cells. Moreover, GOx exhibited higher catalytic activity in the tumor acidic environment but decreased activity under neutral conditions. Furthermore, the stable blood glucose and oxygen saturation of mice and no CO poisoning proved the safety of the nanofactory (Wang et al., 2019c).

The aforesaid studies verify the value of CM@PLGA NPs in cancer treatment. Only when the excellent *in vivo* behavior of CM coat combined with PLGA's inclusiveness of diverse therapeutic molecules, can outstanding antitumor strategies be achieved through compensating for their shortcomings and utilizing their advantages. Also, we believe that cancer vaccines have great developmental prospects. Thus, their combination with immunostimulants or checkpoint inhibitors may pave the way for clinical transformation.

4.2. Cardiovascular diseases

4.2.1. Atherosclerosis

AS is a progressive inflammatory disease characterized by the accumulation of lipids, immune cells, and fiber components in arterial walls (Zhong et al., 2019). The gradual formation of atherosclerotic plaque, sclerosis, and artery stenosis ultimately lead to severe cardiovascular diseases, which account for the leading number of deaths across the world (Wang et al., 2019b). The conventional oral drugs produce

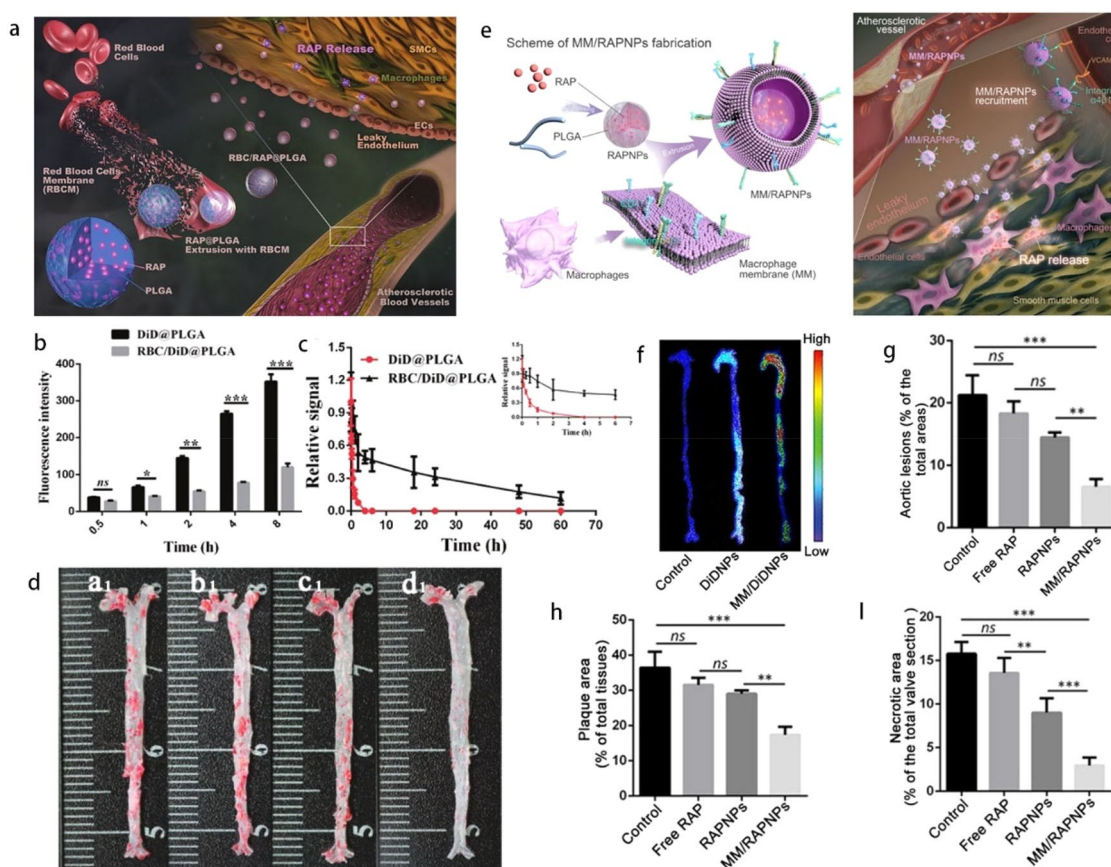


Figure 7. (a) Schematic of RBC/RAP@PLGA for AS treatment. (b) Reduced cellular uptake of NPs in macrophages and (c) prolonged body circulation. (d) The atherosclerotic lesions of aortas from each group (a, Control; b, Free drug; c, RAP@PLGA; d, RBC/RAP@PLGA) (Wang et al., 2019b). Copyright 2019 Wiley-VCH. (e) Schematic of MM/RAPNP for AS treatment. (f) Targeting atherosclerotic plaques. Quantitative analysis of (g) the lesion area, (h) lipid deposition area and (i) necrotic cores of plaque lesions in the cross-sections of the aortic root (Wang et al., 2021). Copyright 2021 IVY Publisher.

adverse reactions due to the nonspecific distribution after their long-term use. However, the advent of CM@PLGA can provide effective countermeasures to these problems.

Rapamycin-loaded RBCM@PLGA nanocomplexes were constructed with a well-defined bio-interface to restrain the progression of AS (Figure 7(a)) (Wang et al., 2019b). Owing to the extensive drug-loading capacity of the PLGA core, the loading rate and encapsulation efficiency of rapamycin (a type of hydrophobic drug) were 7.79% and 84.5%, respectively. After a month of treatment, the necrotic area, collagen, and the numbers of smooth muscle cells were significantly reduced. This result stems from the decreased phagocytosis of nanocomplexes by macrophages, prolonged body circulation, and increased accumulation at the lesion site (Figure 7(b–d)). The same researchers further employed MM-disguised PLGA nanocomplexes (Figure 7(e)) (Wang et al., 2021). Activated ECs in the damaged vessels highly expressed VCAM-1 and secreted chemokines to recruit circulating monocyte macrophages through the specific recognition of integrin $\alpha_4\beta_1$ (Gimbrone & Garcia-Cardena, 2016; Yang et al., 2020). Western blot results confirmed the retention of integrin $\alpha_4\beta_1$ and CD47 on the nanosystem surface. MM decoration inhibited the proinflammatory cytokines secretion as well as the proliferation of macrophages and smooth muscle cells. The atherosclerotic plaques targeting (Figure 7(f)) benefit from EPR effect as well as the specific affinity between integrin $\alpha_4\beta_1$ and VCAM-1 with the lowest atherosclerotic lesions

(6.59%), lipid deposition (17.41%), and necrotic core areas (2.95%) (Wang et al., 2021) (Figure 7(g–i)). Recently, MM co-modified by CD47 and integrin $\alpha_4\beta_1$ was coated onto colchicine-loaded NPs to realize immunophagocytosis escape and more advanced targeting in response to biological signals, thereby exhibiting an excellent antiplaque effect and stable fragile plaques (Li et al., 2022). Sustained-release characteristics inherited from PLGA, effective targeted capacity, and satisfactory safety of long-term administration were deemed advantageous for chronic disease management (Yang et al., 2020).

4.2.2. Ischemic stroke

Ischemic stroke is generally secondary to the AS, leading to cerebrovascular obstruction or stenosis (Bradberry et al., 2004). Therapeutic quantity of drugs crossing BBB is essential for inducing precise pharmacological action. Taking advantage of the ischemic brain-targeting ability of neural SCs (NSCs), glyburide-loaded PLGA NPs were encapsulated with the NSC membranes. The resultant enhanced transmission to the ischemic brain depended on the CXCR4/SDF-1 axis in the lesion area. CXCR4-overexpressed NSC membrane further significantly improved the stroke targeting by 2.1-fold relative to that by the nonfunctional NPs. Especially, in MCAO mice, a 58% reduction was noted in the infarct volume, resulting in improved neurological scores upon i.v. administration (5 $\mu\text{g}/\text{kg}$ glyburide, 3 doses) (Ma et al., 2019). Additional

endpoint measures, such as oxidative stress and behavioral deficits, could be examined whether there are specific pathways of effect (Alkaff et al., 2020). Considering the complexity of stroke pathology, diverse interventions may be available. This targeted drug delivery combined with the clinical gold standard tissue plasminogen activator is expected to prolong the therapeutic time-window of the latter.

4.2.3. Myocardial infarction

For treating myocardial infarction, a synthetic SC-mimicking NPs (CMMP) consist of SCs membrane and secretome from cardiac SCs in PLGA core to supply safe building modules for controlled release. CMMPs have a size and surface antigens consistent with true cardiac SCs, and remain stable of membrane coating even after freeze-lysis process. By superior binding with newborn cardiomyocytes *in vitro*, CMMP robustly promoted the proliferation, division, contraction, and rolling movement of cardiomyocytes. After intramyocardial injection, the majority of CMMPs remained in the heart and robustly boosted the cardiac functions, with the highest left ventricular ejection fractions achieved at 4 weeks. Unlike genuine SCs, CMMP exhibited greater safety profiles without evoking T-cell infiltration (Tang et al., 2017). Accumulating evidence suggests that SCs exert their function through the paracrine mechanism and the membrane-based contact between SCs and recipient cells (Hodgkinson et al., 2016). This off-the-shelf SCs imitator offers advantages over live cells in terms of the

ease of storage, greater stability, and less immunogenicity and tumorigenicity, making it conducive for clinical translation. Furthermore, this platform can be extended to the regeneration of other organ functions.

4.3. Inflammatory diseases

Inflammation is an innate protective response against harmful triggers, whereas abnormal inflammation culminates in many chronic and degenerative diseases (Karin & Clevers, 2016). Autoimmune diseases such as rheumatoid arthritis and gastroenteritis have a fundamental connection with inflammation (Jin et al., 2018). The biomimetic carriers harness inflammatory targeting immune CM upon coating on the PLGA inner core to form a spherical core/shell structure and exhibit right-side-out orientation for better membrane protein exposure, thereby offering a function-driven and beneficial effect toward disease treatment.

4.3.1. Rheumatoid arthritis

Rheumatoid arthritis (RA) is a chronic autoimmune disease and the primary cause of joint damage and disability (Smolen et al., 2016). A neutrophil-like NP with successful translocation of the key surface antigens has been implicated in RA management (Zhang et al., 2018a). Mimicking the source cells enabled neutrophil-NPs target inflamed cells, inhibition of

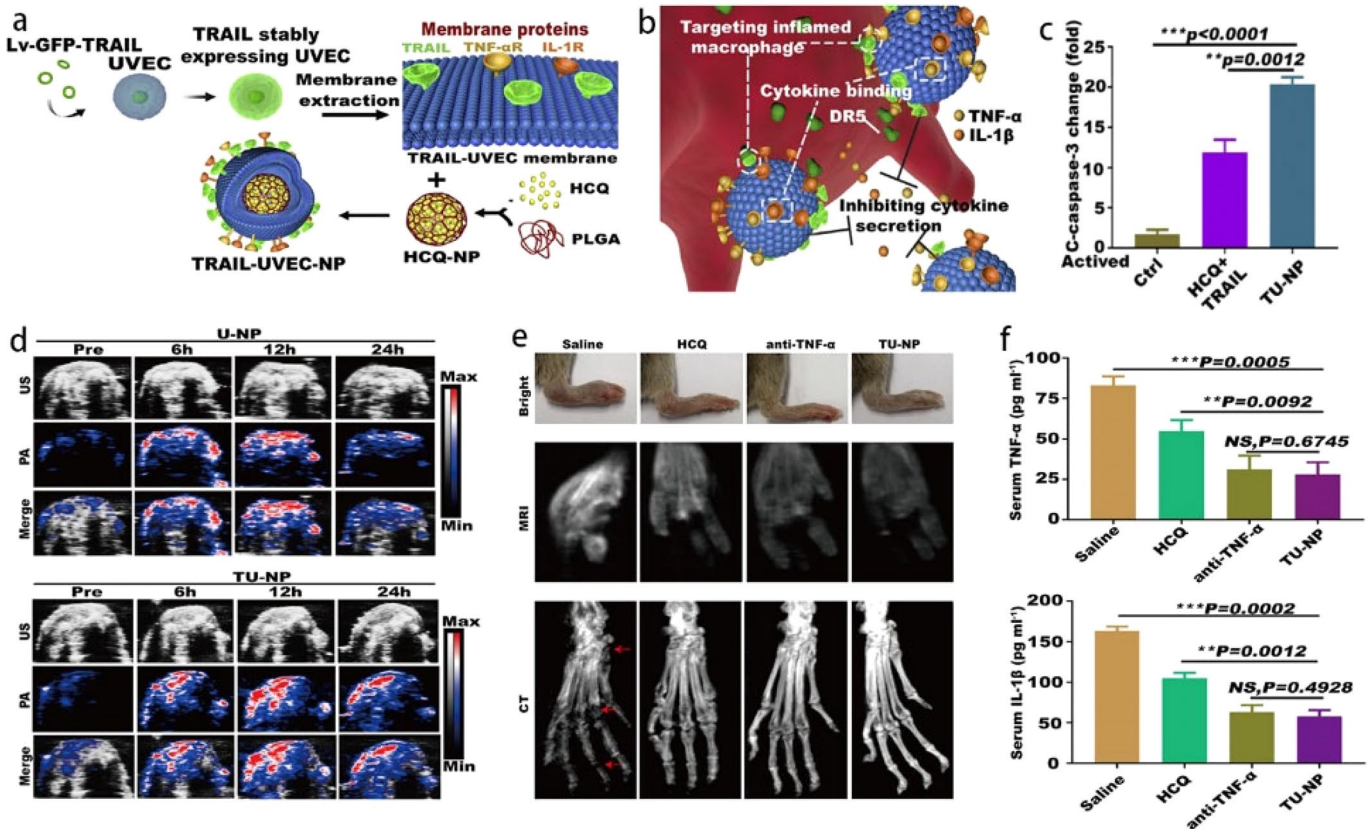


Figure 8. (a) Schematic illustration of TU-NPs and (b) targeting mechanisms to inhibit inflammatory cytokines. (c) The boosted cleaved caspase-3 indicates M1 macrophages apoptosis. (d) The penetration of NPs into the inflamed paws under US and PA after 12h *i.v.* injection. (e) TU-NPs improve the prophylactic effect in early-stage RA with enhanced bone protection and (f) decreased serum pro-inflammation cytokines. The red arrow represents the erosion of joints (Shi et al., 2020). Copyright 2020 Elsevier.

HUVEC activation, and neutralization of pro-arthritis factors that otherwise recruited endogenous neutrophils for inflammation cascade. Moreover, more than 80% cartilage was maintained attributable to the stronger cartilage penetration than RBC-NPs. Finally, in an arthritic mouse model, significant joint damage was halted and a systemic therapeutic response following a prophylactic regimen was evoked.

In another study, platelet-mimetic NPs (PNPs) were developed for FK506 (an immunosuppressant agent) delivery showcasing a tremendously high encapsulation efficiency of 96.7% (He et al., 2018). The improved interaction of PNPs with synoviocytes could be due to the affinity between GPVI receptors on the membrane with collagen IV. After systemic administration in collagen-induced arthritis mice, FK506-PNPs exhibited a high accumulation in inflamed joints (2.1-fold more than that by bare NPs), as well as a notable anti-arthritis effect. Recently, TRAIL-anchored HUVEC membrane-coated PLGA NPs (TU-NPs) were designed for hydroxychloroquine delivery and sustained release in inflamed tissues (Figure 8(a)). The release rate of drugs in TU-NPs was lower than that in bare NPs, which could be due to the coating of CM on the PLGA NPs. The sustained drug-release feature could decrease the drug leakage and extend the circulation time *in vivo*. TRAIL targeted DR5-overexpressed activated M1 macrophages at the inflammation site and induced their apoptosis, meanwhile, the HUVEC membrane could neutralize the inflammatory factors (Figure 8(b,c)). Photoacoustic (PA) and US assay revealed greater accumulation and penetration into the inflamed paws, which was approximately 2-times deeper than those by U-NPs after 12 h of i.v. injection (Figure 8(d)). In *in vivo* therapeutic effect study, magnetic resonance imaging (MRI) and CT results revealed optimal joint and bone protection in mice along with an effective prophylactic effect with decreased serum pro-inflammation cytokines at the early stage of RA (Figure 8(e,f)) (Shi et al., 2020).

4.3.2. Ulcerative colitis

Ulcerative colitis (UC) is a non-curable and easy relapsing inflammatory bowel disease that heavily compromises a patient's quality of life (Hendriksen et al., 1985). To reduce the symptoms and alleged suffering, the patients have to follow the prescription of daily administration of glucocorticoids and immunosuppressive agents (Neurath, 2017); however, the systemic adverse side of conventional drugs over long-term medication cannot be ignored.

S100A9 is a molecular target that can recruit macrophages and polarize locally into the M1 type in UC patients (Zhang et al., 2015). Li et al. constructed a stable oral nanomedicine, MM-PLGA-TAS, composed of TLR4-overexpressed MMs and tasquinimod (TAS, an S100A9 inhibitor) encapsulated in PLGA with a sustained-release profile. Because of macrophage-homing as well as the specific affinity of TLR4 for S100a9, MM-PLGA-TAS exhibited strong accumulation in RAW264.7 cells with an inflammatory phenotype and dramatically high enrichment in inflamed colonic tissues. Oral administration of MM-PLGA-TAS (10 mg/kg TAS equivalent) in colitis mice led to the longest colon length and least inflammatory response. Tissue TUNEL assays revealed alleviation of apoptosis with the

downregulation of the P65 and Stat3 signaling pathways by enriched TAS (Li et al., 2021c). This oral biocompatible formulation is an ideal paradigm for UC management for its convenient, secure, and effective therapy considering that there is no radical solution for UC yet.

4.4. Detoxication

Nanosponges, which consist of a biofilm surface and a polymer core, are a novel therapeutic modality that makes full use of nature's mechanisms for detoxication. For instance, RBCM-derived nanosponges can neutralize a broad spectrum of pore-forming toxins. In addition, the increased surface-to-volume ratio of the membrane material after coating on PLGA NPs further contributes to more efficient toxin neutralization. In fact, the 'toxin decoy effect' has expanded to the field of antipathogen, antichemotoxic agents, and other pathological molecules.

4.4.1. Antibacterial infections

Sepsis is triggered by the uncontrolled systematic inflammatory responses to the systemic spread of endotoxins from bacterial (Yaroustovsky et al., 2013). Macrophage-like NPs (MΦ-NPs) retained inherent epitopes not only specifically bind and neutralize endotoxins LPS but also sequester proinflammatory cytokines, which ultimately quench the dramatic immune dysregulation relative to that by RBC-NPs or PEG-NPs (Thamphiwatana et al., 2017). In a lethal challenge, *Escherichia coli* bacteremia model, i.v. injection of MΦ-NPs ultimately conferred a significant survival benefit and reduction of bacterial burden in the blood and spleen of the host. In another study, gastric epithelial CM@PLGA loading an antibiotic defeated *Helicobacter pylori*-infection based on the pathogen-host inherent adhesion mechanism. A superior anti-*H. pylori* efficacy of approximately three orders of magnitude reduction of the bacterial burden was recorded after an oral administration of clarithromycin (30 mg/kg) once a day for five consecutive days (Angsantikul et al., 2018).

Multiple resistance of bacteria is a mounting trouble in clinics. Tedizolid phosphate (TR-701) is a new antibiotic that has been approved for acute skin infections caused by MASR infection, but lacks an effective dosage form. The new formulation of TR-701-loaded RBCM@PLGA NPs significantly reduced the RBCs hemolysis rate of the exotoxin (Wu et al., 2021). In an MRSA USA 300-wound infection model, the best wound healing and MRSA growth inhibition were obtained through the coordinated antibacterial efficacy of both RBCM and TR-701.

Recently, RBCM-cloaked dihydroartemisinin NPs effectively targeted *Plasmodium*-infected RBCs for enhanced antimalarial efficacy, with a higher inhibition ratio and a substantially lower ED 90 (Zuo et al., 2022). Generally, this nanosponge preserved the toxin-binding capacity from the original cells and enhanced the delivery of the antibiotic. The responsive release of antibiotics in the infection spot may achieve a more robust antibacterial efficacy with reduced drug resistance.

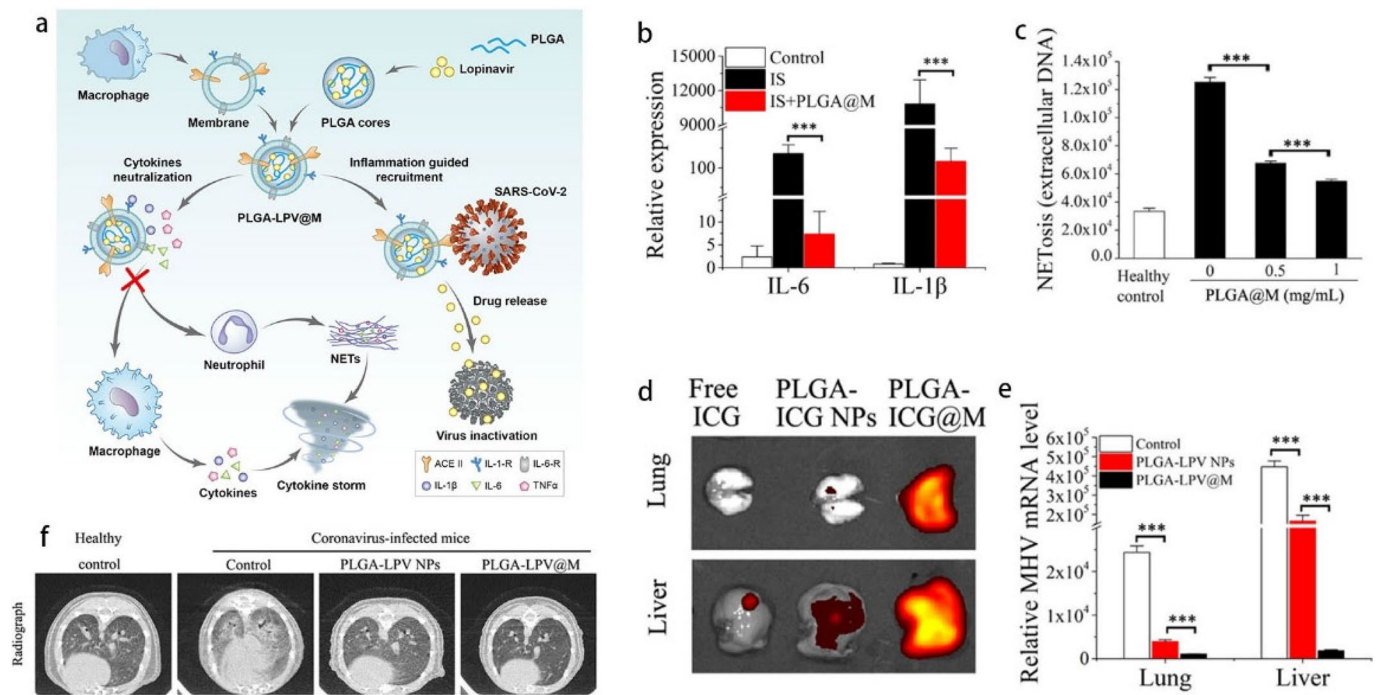


Figure 9. (a) Schematic illustration of PLGA-LPV@M for anti-inflammation and targeted antiviral treatment in COVID-19. (b) PLGA@M reduce the expression of IL-6 and IL-1 β in macrophages stimulated with virus infected supernatant. (c) NETosis in neutrophils induced by COVID-19 patient serums was quantified after treatment with PLGA@M. (d) Fluorescence signal in liver and lung of coronavirus infected mouse. (e) The viral loads of lung and liver in coronavirus infectious mice after treated with the NPs. (f) Radiography analysis of lung with different treatments (Tan et al., 2021). Copyright 2020 Springer Nature.

4.4.2. Antiviral infections

The COVID-19 pandemic, caused by SARS-CoV-2 infection (Finkel et al., 2021), has unfolded into a serious public health crisis and hampered the treatment of other diseases as well. In severe cases, cytokine storm syndrome (CSS) is the leading cause of high mortality (Moore & June, 2020). However, so far, coronavirus remains mutable and wanton, making it of paramount importance to clarify the complex pathogenesis and develop effective treatment strategies urgently.

A focus on the host cells invaded by virus led to the development of innovative nanosponge-inherited host CM protein receptors such as ACE II and CD147, that response for virus entering hosts. Human lung epithelial type-II cells and human macrophage nanosponges with the right-side-out membrane protein orientation driven by the repulsion between the electronegative PLGA cores and the extracellular membrane were deemed crucial for binding virus. Lung acute toxicity test and normal blood parameters confirmed their short-term safety. Two types of nanosponges neutralized authentic SARS-CoV-2 in a dose-dependent manner *in vitro* and performed much better than the RBCM nanosponges. Finally, the authors argued that MM nanosponges may be superior to lung epithelial nanosponges given the central role of macrophages in early viral infection and late hyperinflammation (Zhang et al., 2020a).

In addition, excessive neutrophil extracellular traps (NETs), the thread-like extracellular structures for eradicating virus, also led to CSS (Tan et al., 2021). A nano-sized macrophage mimic (PLGA@M) with excellent colloidal stability consisted of MM shell and PLGA core for drug loading (Figure 9(a)). The surface receptors inherited from MMs could decrease proinflammatory cytokines IL-6 (100-fold) and IL-1 β (10-fold)

for suppressing the activation of immune cells (Figure 9(b)). Together, PLGA@M also significantly reduced the formation of NETs induced by COVID-19 patient serum (Figure 9(c)). These two aspects finally alleviated the progression of CSS. The biodistribution indicated that PLGA-ICG@M preferred to accumulate at the inflammation sites in surrogated coronavirus-infected mice (Figure 9(d)). Furthermore, the lipophilic lopinivir (LPV) was loaded in PLGA for stabilization in aqueous medium. ACE II on MM could specifically target the SARS-CoV-2 spike protein, directly capture virus, and prominently guide LPV toward them. In accordance, PLGA-LPV@M exhibited excellent synergistic effects of inflammation alleviation, survival rate improvement, and viral load reduction in a mouse model (Figure 9(e,f)) (Tan et al., 2021).

CM-based nanosponges act as baits to neutralize viruses and inflammatory factors and exempt host cells from infection and deterioration. When compared with conventional antiviral drugs, this technology can provide countermeasures that are not limited by virus mutation and possible future virus species as long as the host is the viral target. Moreover, nanosponges can be personalized with different source CM and therapeutic agents for efficient delivery to the hijacked virus. Considering the systemic safety and efficiency, this coordinated strategy can provide strong support for appropriate clinical treatment or better managing future pandemic diseases.

4.4.3. Antichemotoxic agents or other pathological molecules

In addition to the effect on biological pathogens, nanosponge can detoxify organophosphate poison that induces life-threatening neurotoxicity by irreversibly inhibiting the

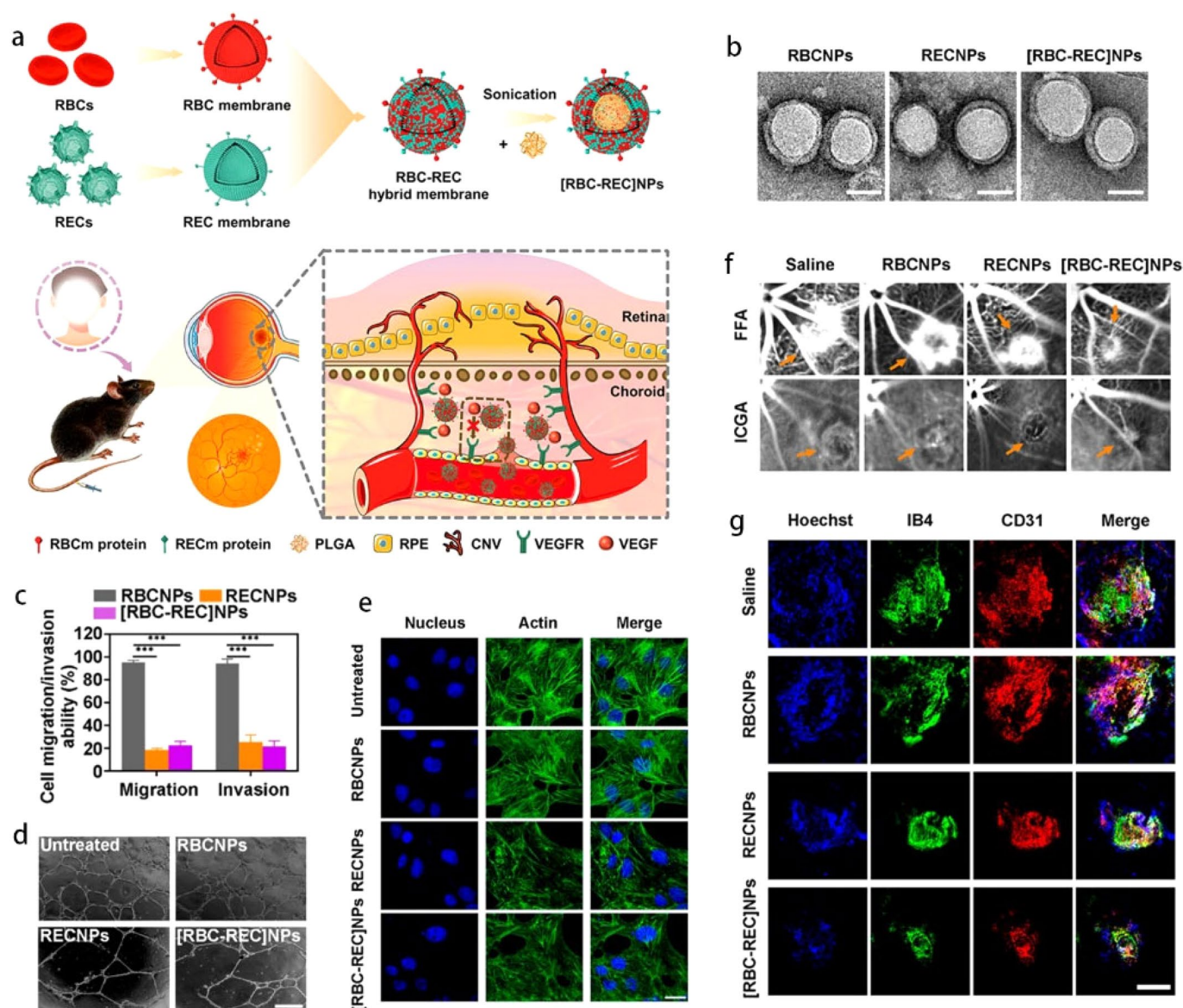


Figure 10. (a) Schematic illustration of [RBC-REC]NPs designed for noninvasive targeted treatment of laser-induced CNV. (b) TEM images. (c) REC migration/invasion ability, (d) capillary tube formations and (e) actin filaments in RECs after incubation with various NPs. (f) Representative fundus photographs of CNV regions in a mouse model. (g) Confocal images of choroid flat mounts after i.v. injections with different treatment. Blue, nucleus; green, CNV lesions; red, ECs. Scale bar, 100 μ m (Li et al., 2021b). Copyright 2021 American Chemical Society.

acetylcholinesterase (AChE) activity. RBCM nanosponge was driven to absorb chlorpyrifos in a dose-dependent manner. In a rabbit model challenged with a lethal dose of chlorpyrifos, the mortality was abruptly decreased and AChE activity was preserved and gradually reactivated by day 4 of the challenge (Altaf et al., 2021).

A recent study reported noninvasive treatment of choroidal neovascularization (CNV) with hybrid retinal endothelial cell (REC) membrane and RBCM ([RBC-REC] NPs) (Figure 10(a)) (Li et al., 2021b). Coating the inner core of PLGA yielded cellular biomimetic NPs with nanoscale spherical core-shell structures of eximious colloidal stability (Figure 10(b)). RBCM reduced NPs phagocytosis *in vivo*, and the rich surface-adhesion molecules in REC membrane enhanced the remarkable self-recognition ability of NPs to host RECs. Moreover, inhibition of the antiangiogenic activity with reduced retinal endotheliocyte migration, capillary tube, and microfilament

formation was validated *in vitro* (Figure 10(c–e)). An effective reduction in CNV leakage in [RBC-REC]NP-treated eyes of laser-induced CNV mouse was achieved with i.v. injection (Figure 10(f,g)). The capability of absorbing proangiogenic factors and blocking their effect on host RECs provide a less invasive and alluring treatment mode, which is better than the conventionally provided invasive intravitreal injection.

4.5. Theranostics

4.5.1. Fluorescence imaging

In addition to its potential for various disease treatments, the bionic nanoplatform is also a prospective candidate for contrast agents *in vivo* imaging and therapeutic diagnosis (Geng et al., 2020). In a past study, DiD-loaded RBCM-functionalized PLGA was used to investigate the distribution and pharmacokinetics *in vivo* (Hu et al., 2011). ICG-loaded NPs

camouflaged by CCM (ICNPs) exhibited excellent fluorescence (FL)/PA imaging dual-mode and thermal responsiveness (Chen et al., 2016). Benefitting from the homologous targeting of CCM, tumor accumulation of ICNPs was 3.1-fold relative to that of bare NPs. High spatial resolution and deep penetration are conducive to real-time monitoring of body distribution. Both H&E staining and blood biochemistry tests indicated good biocompatibility *in vivo*. Recently, brain metastatic MDA-MB 831 CM-cloaked PLGA NPs (CCNP) loaded IR 780-I as an *in vivo* imaging agent to cross the BBB (Kumar et al., 2019). The fluorescence intensity of CCNP in the brain was twice greater than that of mPEG-PLGA until 48 h. Notably, the presence of brain metastatic CM protein enables NPs to breach the BBB and enhances brain retention.

4.5.2. Ultrasound imaging

US imaging is widely applied for medical diagnosis, offering the merits of good directivity, deep tissue penetration, better safety, and economically sounder. PLGA has been used as a US-contrast agent. When compared with the commercial lipid microbubbles, PLGA microbubbles present with better stability, high drug-loading capacity, and longer imaging window (Song et al., 2018). The integration of biomimetic profile of CM and high drug encapsulation efficiency of PLGA can realize accurate targeting to the lesion site and superior US performance. PM enables porous PLGA microbubbles filled with perfluoropropane to precise target early myocardial ischemia-reperfusion injury. The relatively higher specificity and enhanced accumulation in the risk area contribute to the significantly higher signal intensity (Xu et al., 2021).

4.5.3. Photoacoustic imaging

PA imaging, a fast-developing noninvasive image strategy that offers a high contrast rate and penetration depth, has garnered considerable attention recently. However, some imperfections continue to exist, including the poor targeting capacity and easy clearance of the PA contrast agent from the systemic circulation. A novel nanoprobe DiR-loaded CCM@PLGA (MPD), was constructed. High DiR-loading capacity and the whole proteins from source cells were kept. In living tumor xenografted mice, when compared with DiR and DiR-loaded PLGA, MPD presented with the strongest PA signals in tumor and the least liver and spleen accumulation with a longer circulation lifetime allowing for deep tissue imaging (Huang et al., 2021).

4.5.4. Magnetic resonance imaging

MRI contrast agent, lipid-chelated gadolinium, was inserted into the lipid bilayer of PM-coated PLGA NPs (PNP) for AS detection. PNP can bind foam cells, collagen, and activated ECs when compared to PEG-modified or RBCM-coated NPs. In addition to mature AS, it targets pre-atherosclerotic lesions. Thus, it can be said that enhanced accumulation of gadolinium at the plaque regions can enable live detection of AS (Wei et al., 2018).

Neuroinflammation is involved in brain damage caused by stroke. Selective and accurate monitoring is, thus, a

prerequisite for corresponding therapy. Recently, an innovative magnetic nanoprobe (NMNP) for enhanced neuroinflammation imaging was reported (Tang et al., 2021). Briefly, superparamagnetic iron oxide-loaded PLGA nanocore was coated with a biomimetic shell of neutrophil membrane. The successful transfer of adhesion molecules and CD47 from neutrophils granted NMNPs with an excellent binding affinity to activate the endothelium and avoid immune phagocytosis, respectively. After the *i.v.* administration in tMCAO mice, NMNP could target inflamed cerebral microvessels, and the fluorescence intensity was 7.9-fold higher than that of the RMNP group. Indeed, enhanced MRI contrast with the largest number of dark voxels in the ischemic region was detected on intravital imaging, which indicates an alluring prospect for neuroinflammation MRI.

Each imaging method has its limitations, so integrating different technologies in one system can achieve more informative and precise images by complementing their strengths. An A549CM-coated nanoprobe was delicately designed to achieve mutual complementary ¹⁹F MR/PA/FL tri-modality imaging (Li et al., 2020). Thanks to homologous targeting endowed by A549CM, first, rapid real-time scanning with high sensitivity can be performed by FL imaging, after which ¹⁹F MRI can be conducted to reveal more precise anatomical information of tumors with a higher signal to noise ratio, and finally, PA imaging can vividly demonstrate the heterogeneous intratumoral distribution of NPs with a high spatial resolution. Alternatively, multifunctional bionic 'nanoplatelets', consisting of PM coat and PLGA core coloaded with nanocarbons (CNs, a PA imaging contrast), DOX, and perfluoropentane (PFP), were specifically tailored for early diagnosis and therapy of tumor (Li et al., 2021a). Under 808-nm 2.0W/cm² NIR and 5-min irradiation, NPs could reach 67.6°C due to the desirable photothermal conversion property of CNs. The local hyperthermia initiated the optical droplet vaporization of PFP, and the liquid-gas change remarkably enhanced the US imaging. Moreover, the combined cavitation effect with hyperthermia and the enhanced phase changed fluidity of PLGA, resulted in the release of 77.76% DOX. Through the specific binding of P-selectin with CD44, targeted NPs revealed 4.56-fold higher tumor accumulation compared to bare NPs. Finally, under the multimodal PA/FL/US image guide, 'nanoplatelets' displayed an outstanding synergistic PTT-chemo therapy considering that the tumors were completely ablated.

The aforementioned examples provide a new feasible strategy for image-guided therapy and demonstrate a valid multimodal theranostic system that combines an imaging technique with the delivery of therapeutic agents to maximize drug efficacy. Moreover, the natural membrane-coating technology makes the detection system biocompatible, immune-exempted, and offering more selective and precise outcomes.

5. Conclusion and perspectives

The present article comprehensively introduces the recent advancements in the CM@PLGA biomimetic system from the

perspective of CM origin, membrane vesicle modification, and applications of disease treatment and diagnosis. The last decade witnessed a boom of CM-camouflaged techniques along with the exploration of different sources of CM. Further flexible modification on membrane vesicles has realized the expected function enhancement on the premise of not subverting their biological functions. Genetic engineering preserves CM functions to their maximum extent; lipid insertion with an abundant source of ligand is most labor-saving and hybrid membranes can optimize diverse combinations. Innate lesion-homing capabilities of CM provide excellent drug delivery and multimodal diagnosis across varied fields, including cancer, immune diseases, and infectious diseases. For instance, integration of different mechanisms such as immunotherapy, light therapy, and ferroptosis can overcome tumor resistance (Wang et al., 2022b). Notably, the bionic system with an increased surface area upon the coating on PLGA core is more conducive for exposure and stretching of antigen or receptor-binding protein and shows great talents in immunoregulation, anti-inflammatory, pathological molecular blockade, and nanosponge detoxification. The synergistic decoy effect for virus captures and pro-inflammatory factors neutralization provides a new treatment model for wanton capricious COVID-19 or the inevitable future epidemics. Recently, scientists have pioneered the existence of tumor-resident intracellular microbiota as accomplices of metastasis (Fu et al., 2022). Accordingly, targeting them in primary or circulating tumor cells seems to be an intriguing attempt to impede metastasis. In addition, further cutting-edge advancements in disease pathology are expected to give rise to opportunities for different disease interventions such as immune diseases antiphospholipid syndrome in gynecopathy due to the ubiquitous intercellular interaction.

PLGA-based preparations have been applied in clinics for decades, thanks to their superior safety, biodegradability, and outstanding diverse drug-loading tolerance. When compared to other nanocarriers, such as liposomes or micelles, prolonged dosing interval conferred by the unique sustained release mechanism of PLGA formulations has been deemed a critical requirement for chronic diseases. More excitingly, the desired degradation rate and drug release rate of PLGA nanocarriers can be achieved by regulating the ratio of lactide to glycolide polymer, molecular weight, and formulation method. The advent of nature-inspired CM-camouflaged technique by transferring the cell's dialogue mechanism and surface properties to nanocarriers is indeed a new revolution. Results have shown that CM coating prevents the initial burst release, endows PLGA NPs with excellent stealth features, facilitates immune escape and navigation to the site of interest, and improves drug therapy index by minimizing their off-target toxicity. Moreover, PLGA provides certain support to the CM and improves the stability of the entire nanosystem in blood circulation. The dual drug-loading nanosystem combines the advantages of CM and PLGA and meets some special drug requirements by realizing the sequential release of the drugs. Furthermore, CM@PLGA has demonstrated great advantages in gas delivery, making it a potential nanocarrier in the field of gas therapy. The attractiveness of this platform is not limited to the field of drug delivery. In contrast to

whole-cell carriers, they not only exhibit cell-like behavior by the inherited membrane functional proteins or antigens but also overcomes the problem of storage, latent contamination, and clogging of the blood vessels. Unlike living cells, 100–200 nm-range size upon the CM coating onto PLGA NPs is more capable to penetrate and cross the tissue barriers. Generally, CM narrows the gap between the synthetic material PLGA and the organisms, meanwhile, PLGA is the most direct bridge to clinical transformation for CM-coating technology. In conclusion, CM@PLGA can overcome the flaws of CM and PLGA in drug delivery. The combination of CM and PLGA, thus, enables relatively more efficient drug delivery and safer disease treatment.

Despite the enthusiasm for its delightful efficiency, the proposed platform is still in its infancy, and there are some issues demanding solutions before appropriate clinical applications. The first requirement is the acquisition and quality control of CM. Autologous cells are reliable for personalized therapy, albeit their time-consuming feature may delay a patient's 'timely' treatment. Xenogeneic cells need to be strictly matched and allergens and tumorigenic factors should be removed from CCM. The homogeneity of the vesicles also warrants consideration, as batch differences continue to exist due to the inconsistent expression of the membrane proteins in different cell cycles (Le et al., 2021). Second, the preparation process needs further optimization. The integrity of the CM after extraction with the least membrane protein function destruction and the coating ratio on PLGA, especially for non-nucleated cells with limited sources have not been mentioned in most of the past studies. Moreover, the most widely used extrusion-coating method has not been deemed conducive to industrialization, often resulting in batch differences due to the manual multistep coating process. It is, therefore, necessary to develop uniform standards for the preparation and storage processes. Third, the *in vivo* behavior and safety aspects of the vector warrant further scrutiny, especially relating to the manner of its entrance into target cells and drug-release behavior, the rupture time of the membrane coat in body's circulation, and the metabolic mechanism. Related studies have mainly investigated the curative efficacy and side effects on major organs. Nevertheless, as CM is a complex communicator, the least impact on the normal physiological functions, such as PM-based carrier, not affecting the hemostatic function should be reported. In addition, the immunogenicity of allogeneic cells cannot be ignored, while gene-editing techniques may be available to eliminate the immunogenic membrane proteins (Xu et al., 2019). Although the biosafety of PLGA molecules is high, the embolic toxicity and inflammatory response of PLGA should be evaluated after being prepared into micro-nano sizes. Finally, its effectiveness is depended on the source animals, and hence species variation between mice and humans cannot be ignored. Nevertheless, extensive clinical evaluations need to be evaluated in detail. Presently, the RBCM-camouflaged PLGA platform is under preparation for clinical trials. Considering its unprecedented advantages over traditional synthetic material nanotechnology, CM@PLGA biomimetic platforms are bound to demonstrate important implications for human disease interventions.

Disclosure statement

The authors declare that there is no conflict of interest.

Funding

This study was financially supported by the National Natural Science Foundation of China (81802587, 82103505, and 82071616).

ORCID

Mengdan Zhao  <http://orcid.org/0000-0002-1491-0588>

References

- Alkaff SA, Radhakrishnan K, Nedumaran AM, et al. (2020). Nanocarriers for stroke therapy: advances and obstacles in translating animal studies. *Int J Nanomed* 15:445–64.
- Allen C, Evans JC. (2020). 'Hip to be square': designing PLGA formulations for the future. *J Control Release* 319:487–8.
- Altaf S, Muhammad F, Aslam B, et al. (2021). Cell membrane enveloped polymeric nanosponge for detoxification of chlorpyrifos poison: in vitro and in vivo studies. *Hum Exp Toxicol* 40:1286–95.
- Angsantikul P, Thamphiwatana S, Zhang QZ, et al. (2018). Coating nanoparticles with gastric epithelial cell membrane for targeted antibiotic delivery against *Helicobacter pylori*. *Adv Therap* 1:1800016.
- Anwar M, Muhammad F, Akhtar B, et al. (2021). Outer membrane protein-coated nanoparticles as antibacterial vaccine candidates. *Int J Pept Res Ther* 27:1689–97.
- Bose RJ, Lee S-H, Park H. (2016). Lipid-based surface engineering of PLGA nanoparticles for drug and gene delivery applications. *Biomater Res* 20:34.
- Bose RJ, Kim BJ, Arai Y, et al. (2018). Bioengineered stem cell membrane functionalized nanocarriers for therapeutic targeting of severe hind-limb ischemia. *Biomaterials* 185:360–70.
- Bradberry JC, Fagan SC, Gray DR, et al. (2004). New perspectives on the pharmacotherapy of ischemic stroke. *J Am Pharm Assoc* (2003) 44:S46–S56.
- Cai JX, Liu JH, Wu JY, et al. (2022). Hybrid cell membrane-functionalized biomimetic nanoparticles for targeted therapy of osteosarcoma. *Int J Nanomedicine* 17:837–54.
- Chen HY, Deng J, Wang Y, et al. (2020a). Hybrid cell membrane-coated nanoparticles: a multifunctional biomimetic platform for cancer diagnosis and therapy. *Acta Biomater* 112:1–13.
- Chen S, Ren YJ, Duan P. (2020b). Biomimetic nanoparticle loading obataclax mesylate for the treatment of non-small-cell lung cancer (NSCLC) through suppressing Bcl-2 signaling. *Biomed Pharmacother* 129:110371.
- Chen Y, Shen X, Han SL, et al. (2020c). Irradiation pretreatment enhances the therapeutic efficacy of platelet-membrane-camouflaged anti-tumor nanoparticles. *J Nanobiotechnol* 18:101.
- Chen Z, Zhao PF, Luo ZY, et al. (2016). Cancer cell membrane-biomimetic nanoparticles for homologous-targeting dual-modal imaging and photothermal therapy. *Acs Nano* 10:10049–57.
- Chen ZH, Wang WT, Li YS, et al. (2021). Folic acid-modified erythrocyte membrane loading dual drug for targeted and chemo-photothermal synergistic cancer therapy. *Mol Pharm* 18:386–402.
- Cui YX, Sun JJ, Hao WY, et al. (2020). Dual-target peptide-modified erythrocyte membrane-enveloped PLGA nanoparticles for the treatment of glioma. *Front Oncol* 10:563938.
- Dash P, Piras AM, Dash M. (2020). Cell membrane coated nanocarriers - an efficient biomimetic platform for targeted therapy. *J Control Release* 327:546–70.
- De La Harpe KM, Kondiah PPD, Choonara YE, et al. (2019). The hemocompatibility of nanoparticles: a review of cell-nanoparticle interactions and hemostasis. *Cells* 8:1209.
- Dehaini D, Wei XL, Fang RH, et al. (2017). Erythrocyte-platelet hybrid membrane coating for enhanced nanoparticle functionalization. *Adv Mater* 29:1606209.
- Fan ZY, Li PY, Deng JJ, et al. (2018). Cell membrane coating for reducing nanoparticle-induced inflammatory responses to scaffold constructs. *Nano Res* 11:5573–83.
- Fang RH, Kroll AV, Gao WW, et al. (2018). Cell membrane coating nanotechnology. *Adv Mater* 30:1706759.
- Finkel Y, Mizrahi O, Nachshon A, et al. (2021). The coding capacity of SARS-CoV-2. *Nature* 589:125–30.
- Fu AK, Yao BQ, Dong TT, et al. (2022). Tumor-resident intracellular microbiota promotes metastatic colonization in breast cancer. *Cell* 185:1356–72.
- Gao C, Huang QX, Liu CH, et al. (2020a). Treatment of atherosclerosis by macrophage-biomimetic nanoparticles via targeted pharmacotherapy and sequestration of proinflammatory cytokines. *Nat Commun* 11:2622.
- Gao CH, Chu XY, Gong W, et al. (2020b). Neuron tau-targeting biomimetic nanoparticles for curcumin delivery to delay progression of Alzheimer's disease. *J Nanobiotechnol* 18:71.
- Gao M, Hu AY, Sun XQ, et al. (2017a). Photosensitizer decorated red blood cells as an ultrasensitive light responsive drug delivery system. *ACS Appl Mater Interfaces* 9:5855–63.
- Gao M, Liang C, Song XJ, et al. (2017b). Erythrocyte-membrane-enveloped perfluorocarbon as nanoscale artificial red blood cells to relieve tumor hypoxia and enhance cancer radiotherapy. *Adv Mater* 29:1701429.
- Gao Y, Zhu Y, Xu XP, et al. (2021). Surface PEGylated cancer cell membrane-coated nanoparticles for codelivery of curcumin and doxorubicin for the treatment of multidrug resistant esophageal carcinoma. *Front Cell Dev Biol* 9:688070.
- Geng XR, Gao DY, Hu DH, et al. (2020). Active-targeting NIR-II phototheranostics in multiple tumor models using platelet-camouflaged nanoprobe. *ACS Appl Mater Interfaces* 12:55624–37.
- Gimbrone MA, Garcia-Cardena G. (2016). Endothelial cell dysfunction and the pathobiology of atherosclerosis. *Circ Res* 118:620–36.
- Glinsky VV, Huflejt ME, Glinsky GV, et al. (2000). Effects of Thomsen-Friedenreich antigen-specific peptide P-30 on beta-galactoside-mediated homotypic aggregation and adhesion to the endothelium of MDA-MB-435 human breast carcinoma cells. *Cancer Res* 60:2584–8.
- Gong CA, Yu XY, You BM, et al. (2020). Macrophage-cancer hybrid membrane-coated nanoparticles for targeting lung metastasis in breast cancer therapy. *J Nanobiotechnology* 18:92.
- Gou SS, Liu WW, Wang S, et al. (2021). Engineered nanovaccine targeting Clec9a(+) dendritic cells remarkably enhances the cancer immunotherapy effects of STING agonist. *Nano Lett* 21:9939–50.
- Guo K, Liu YX, Tang LR, et al. (2022). Homotypic biomimetic coating synergizes chemo-photothermal combination therapy to treat breast cancer overcoming drug resistance. *Chem Eng J* 428:131120.
- Han SL, Wang WJ, Wang SF, et al. (2019). Multifunctional biomimetic nanoparticles loading baicalin for polarizing tumor-associated macrophages. *Nanoscale* 11:20206–20.
- Han ZW, Lv WX, Li YK, et al. (2020). Improving tumor targeting of exosomal membrane-coated polymeric nanoparticles by conjugation with aptamers. *ACS Appl Bio Mater* 3:2666–73.
- Hao XF, Li Q, Wang HN, et al. (2018). Red-blood-cell-mimetic gene delivery systems for long circulation and high transfection efficiency in ECs. *J Mater Chem B* 6:5975–85.
- He YW, Li RX, Liang JM, et al. (2018). Drug targeting through platelet membrane-coated nanoparticles for the treatment of rheumatoid arthritis. *Nano Res* 11:6086–101.
- Hendriksen C, Kreiner S, Binder V. (1985). Long term prognosis in ulcerative colitis based on results from a regional patient group from the county of Copenhagen. *Gut* 26:158–63.
- Hodgkinson CP, Bareja A, Gomez JA, et al. (2016). Emerging concepts in paracrine mechanisms in regenerative cardiovascular medicine and biology. *Circ Res* 118:95–107.
- Hu C, Lei T, Wang Y, et al. (2020). Phagocyte-membrane-coated and laser-responsive nanoparticles control primary and metastatic cancer by inducing anti-tumor immunity. *Biomaterials* 255:120159.

- Hu CMJ, Fang RH, Wang KC, et al. (2015). Nanoparticle biointerfacing by platelet membrane cloaking. *Nature* 526:118–21.
- Hu CMJ, Zhang L, Aryal S, et al. (2011). Erythrocyte membrane-camouflaged polymeric nanoparticles as a biomimetic delivery platform. *Proc Natl Acad Sci USA* 108:10980–5.
- Hu YL, Fu YH, Tabata Y, et al. (2010). Mesenchymal stem cells: a promising targeted-delivery vehicle in cancer gene therapy. *J Control Release* 147:154–62.
- Huang X, Shen A, Peng R, et al. (2021). A novel biomimetic nanoprobe as a photoacoustic contrast agent. *Front Chem* 9:721799.
- Jiang T, Zhang B, Zhang L, et al. (2018). Biomimetic nanoparticles delivered hedgehog pathway inhibitor to modify tumour microenvironment and improved chemotherapy for pancreatic carcinoma. *Artif Cells Nanomed Biotechnol* 46:1088–101.
- Jin JF, Krishnamachary B, Barnett JD, et al. (2019). Human cancer cell membrane-coated biomimetic nanoparticles reduce fibroblast-mediated invasion and metastasis and induce T-cells. *ACS Appl Mater Interfaces* 11:7850–61.
- Jin K, Luo ZM, Zhang B, et al. (2018). Biomimetic nanoparticles for inflammation targeting. *Acta Pharm Sin B* 8:23–33.
- Kang M, Hong J, Jung M, et al. (2020). T-cell-mimicking nanoparticles for cancer immunotherapy. *Adv Mater* 32:2003368.
- Karin M, Clevers H. (2016). Reparative inflammation takes charge of tissue regeneration. *Nature* 529:307–15.
- Kola SM, Choonara YE, Kumar P, et al. (2021). Platelet-inspired therapeutics: current status, limitations, clinical implications, and future potential. *Drug Deliv Transl Res* 11:24–48.
- Kondo K, Kohno N, Yokoyama A, et al. (1998). Decreased MUC1 expression induces E-cadherin-mediated cell adhesion of breast cancer cell lines. *Cancer Res* 58:2014–9.
- Kumar P, V, TreurenT, Ranjan AP, et al. (2019). In vivo imaging and biodistribution of near infrared dye loaded brain-metastatic-breast-cancer r-cell-membrane coated polymeric nanoparticles. *Nanotechnology* 30:265101.
- Kunde SS, Wairkar S. (2021). Platelet membrane camouflaged nanoparticles: biomimetic architecture for targeted therapy. *Int J Pharm* 598:120395.
- Le QV, Lee J, Lee H, et al. (2021). Cell membrane-derived vesicles for delivery of therapeutic agents. *Acta Pharm Sin B* 11:2096–113.
- Lesterhuis WJ, Haanen J, Punt CJA. (2011). Cancer immunotherapy - revisited. *Nat Rev Drug Discov* 10:591–600.
- Li L, Fu J, Wang XY, et al. (2021a). Biomimetic "nanoplatelets" as a targeted drug delivery platform for breast cancer theranostics. *ACS Appl Mater Interfaces* 13:3605–21.
- Li MJ, Xu ZJ, Zhang L, et al. (2021b). Targeted noninvasive treatment of choroidal neovascularization by hybrid cell-membrane-cloaked biomimetic nanoparticles. *ACS Nano* 15:9808–19.
- Li S, Jiang WP, Yuan YP, et al. (2020). Delicately designed cancer cell membrane-camouflaged nanoparticles for targeted F-19 MR/PA/FL imaging-guided photothermal therapy. *ACS Appl Mater Interfaces* 12:57290–301.
- Li YY, Che JY, Chang L, et al. (2022). CD47-and integrin alpha 4/beta 1-comodified-macrophage-membrane-coated nanoparticles enable delivery of colchicine to atherosclerotic plaque. *Adv Healthcare Mater* 11:2101788.
- Li ZS, Zhang XY, Liu C, et al. (2021c). Macrophage-biomimetic nanoparticles ameliorate ulcerative colitis through reducing inflammatory factors expression. *J Innate Immun* 14:380–92.
- Liang N, Ren N, Feng ZC, et al. (2022). Biomimetic metal-organic frameworks as targeted vehicles to enhance osteogenesis. *Adv Healthc Mater* 11:e2102821.
- Liu C, Zhang W, Li YK, et al. (2019). Microfluidic sonication to assemble exosome membrane-coated nanoparticles for immune evasion-mediated targeting. *Nano Lett* 19:7836–44.
- Liu LQ, Wang Y, Guo X, et al. (2020a). A biomimetic polymer magnetic nanocarrier polarizing tumor-associated macrophages for potentiating immunotherapy. *Small* 16:2003543.
- Liu R, An Y, Jia W, et al. (2020b). Macrophage-mimic shape changeable nanomedicine retained in tumor for multimodal therapy of breast cancer. *J Control Release* 321:589–601.
- Liu X, Zhong X, Li C. (2021). Challenges in cell membrane-camouflaged drug delivery systems: development strategies and future prospects. *Chin Chem Lett* 32:2347–58.
- Liu YF, Wen NC, Li K, et al. (2022). Photolytic removal of red blood cell membranes camouflaged on nanoparticles for enhanced cellular uptake and combined chemo-photodynamic inhibition of cancer cells. *Mol Pharm* 19:805–18.
- Luk BT, Fang RH, Hu CMJ, et al. (2016). Safe and immunocompatible nanocarriers cloaked in RBC membranes for drug delivery to treat solid tumors. *Theranostics* 6:1004–11.
- Luk BT, Hu CMJ, Fang RNH, et al. (2014). Interfacial interactions between natural RBC membranes and synthetic polymeric nanoparticles. *Nanoscale* 6:2730–7.
- Luo L, Tang JN, Nishi K, et al. (2017). Fabrication of synthetic mesenchymal stem cells for the treatment of acute myocardial infarction in mice. *Circ Res* 120:1768–75.
- Ma J, Zhang S, Liu J, et al. (2019). Targeted drug delivery to stroke via chemotactic recruitment of nanoparticles coated with membrane of engineered neural stem cells. *Small* 15:1902011.
- Ma JN, Liu FY, Sheu WC, et al. (2020). Copresentation of tumor antigens and costimulatory molecules via biomimetic nanoparticles for effective cancer immunotherapy. *Nano Lett* 20:4084–94.
- Makadia HK, Siegel SJ. (2011). Poly lactic-co-glycolic acid (PLGA) as biodegradable controlled drug delivery carrier. *Polymers (Basel)* 3:1377–97.
- Mao Y, Zou C, Jiang Y, et al. (2021). Erythrocyte-derived drug delivery systems in cancer therapy. *Chin Chem Lett* 32:990–8.
- Mi Y, Hagan CT, Vincent BG, et al. (2019). Emerging nano-/microapproaches for cancer immunotherapy. *Adv Sci (Weinh)* 6:1801847.
- Moore JB, June CH. (2020). Cytokine release syndrome in severe COVID-19. *Science* 368:473–4.
- Morgan RA, Dudley ME, Wunderlich JR, et al. (2006). Cancer regression in patients after transfer of genetically engineered lymphocytes. *Science* 314:126–9.
- Mura S, Nicolas J, Couvreur P. (2013). Stimuli-responsive nanocarriers for drug delivery. *Nat Mater* 12:991–1003.
- Nakki S, Martinez JO, Evangelopoulos M, et al. (2017). Chlorin e6 functionalized theranostic multistage nanovectors transported by stem cells for effective photodynamic therapy. *ACS Appl Mater Interfaces* 9:23441–9.
- Neurath MF. (2017). Current and emerging therapeutic targets for IBD. *Nat Rev Gastroenterol Hepatol* 14:269–78.
- Nitzsche F, Muller C, Lukomska B, et al. (2017). Concise review: MSC adhesion cascade insights into homing and transendothelial migration. *Stem Cells* 35:1446–60.
- Oldenborg PA, Zheleznyak A, Fang YF, et al. (2000). Role of CD47 as a marker of self on red blood cells. *Science* 288:2051–4.
- Oroojalian F, Beygi M, Baradaran B, et al. (2021). Immune cell membrane-coated biomimetic nanoparticles for targeted cancer therapy. *Small* 17:2006484.
- Pandita D, Kumar S, Lather V. (2015). Hybrid poly(lactic-co-glycolic acid) nanoparticles: design and delivery prospectives. *Drug Discov Today* 20:95–104.
- Park K, Skidmore S, Hadar J, et al. (2019). Injectable, long-acting PLGA formulations: analyzing PLGA and understanding microparticle formation. *J Control Release* 304:125–34.
- Rao L, Xia S, Xu W, et al. (2020). Decoy nanoparticles protect against COVID-19 by concurrently adsorbing viruses and inflammatory cytokines. *Proc Natl Acad Sci USA* 117:27141–7.
- Semple JW, Italiano JE, Freedman J. (2011). Platelets and the immune continuum. *Nat Rev Immunol* 11:264–74.
- Shi Y, Xie FF, Rao PS, et al. (2020). TRAIL-expressing cell membrane nanovesicles as an anti-inflammatory platform for rheumatoid arthritis therapy. *J Control Release* 320:304–13.

- Shi YS, Lin G, Zheng HL, et al. (2021). Biomimetic nanoparticles blocking autophagy for enhanced chemotherapy and metastasis inhibition via reversing focal adhesion disassembly. *J Nanobiotechnology* 19:447.
- Smolen JS, Aletaha D, McInnes IB. (2016). Rheumatoid arthritis. *Lancet* 388:2023–38.
- Song RY, Peng C, Xu XN, et al. (2018). Controllable formation of mono-disperse polymer microbubbles as ultrasound contrast agents. *ACS Appl Mater Interfaces* 10:14312–20.
- Sun KJ, Yu WJ, Ji B, et al. (2020a). Saikosaponin D loaded macrophage membrane-biomimetic nanoparticles target angiogenic signaling for breast cancer therapy. *Appl Mater Today* 18:100505.
- Sun X, He GH, Xiong CX, et al. (2021). One-pot fabrication of hollow porphyrinic MOF nanoparticles with ultrahigh drug loading toward controlled delivery and synergistic cancer therapy. *ACS Appl Mater Interfaces* 13:3679–93.
- Sun YX, Zhai WH, Liu XJ, et al. (2020b). Homotypic cell membrane-cloaked biomimetic nanocarrier for the accurate photothermal-chemotherapy treatment of recurrent hepatocellular carcinoma. *J Nanobiotechnol* 18:60.
- Swider E, Koshkina O, Tel J, et al. (2018). Customizing poly(lactic-co-glycolic acid) particles for biomedical applications. *Acta Biomater* 73:38–51.
- Tan QQ, He LJ, Meng XJ, et al. (2021). Macrophage biomimetic nanocarriers for anti-inflammation and targeted antiviral treatment in COVID-19. *J Nanobiotechnol* 19:173.
- Tang CM, Wang QQ, Li KM, et al. (2021). A neutrophil-mimetic magnetic nanoprobe for molecular magnetic resonance imaging of stroke-induced neuroinflammation. *Biomater Sci* 9:5247–58.
- Tang JA, Shen DL, Caranasos TG, et al. (2017). Therapeutic microparticles functionalized with biomimetic cardiac stem cell membranes and secretome. *Nat Commun* 8:13724.
- Thamphiwatana S, Angsantikul P, Escajadillo T, et al. (2017). Macrophage-like nanoparticles concurrently absorbing endotoxins and proinflammatory cytokines for sepsis management. *Proc Natl Acad Sci USA* 114:11488–93.
- Thi TTH, Pilkington EH, Nguyen DH, et al. (2020). The importance of poly(ethylene glycol) alternatives for overcoming PEG immunogenicity in drug delivery and bioconjugation. *Polymers* 12:298.
- Tian H, Luo ZY, Liu LL, et al. (2017). Cancer cell membrane-biomimetic oxygen nanocarrier for breaking hypoxia-induced chemoresistance. *Adv Funct Mater* 27:1703197.
- Wang HJ, Wu JZ, Williams GR, et al. (2019a). Platelet-membrane-biomimetic nanoparticles for targeted antitumor drug delivery. *J Nanobiotechnol* 17:60.
- Wang M, Hu QD, Huang JM, et al. (2022a). Engineered a dual-targeting biomimetic nanomedicine for pancreatic cancer chemoimmunotherapy. *J Nanobiotechnol* 20:85.
- Wang Q, Cheng H, Peng HS, et al. (2015). Non-genetic engineering of cells for drug delivery and cell-based therapy. *Adv Drug Deliv Rev* 91:125–40.
- Wang Y, Zhang K, Li TH, et al. (2021). Macrophage membrane functionalized biomimetic nanoparticles for targeted anti-atherosclerosis applications. *Theranostics* 11:164–80.
- Wang Y, Zhang K, Qin X, et al. (2019b). Biomimetic nanotherapies: red blood cell based core-shell structured nanocomplexes for atherosclerosis management. *Adv Sci (Weinh)* 6:1900172.
- Wang Y, Zhang L, Zhao GS, et al. (2022b). Homologous targeting nanoparticles for enhanced PDT against osteosarcoma HOS cells and the related molecular mechanisms. *J Nanobiotechnol* 20:83.
- Wang YC, Luan ZY, Zhao CY, et al. (2020). Target delivery selective CSF-1R inhibitor to tumor-associated macrophages via erythrocyte-cancer cell hybrid membrane camouflaged pH-responsive copolymer micelle for cancer immunotherapy. *Eur J Pharm Sci* 142:105136.
- Wang YQ, Liu ZY, Wang H, et al. (2019c). Starvation-amplified CO generation for enhanced cancer therapy via an erythrocyte membrane-biomimetic gas nanofactory. *Acta Biomater* 92:241–53.
- Wei XL, Gao J, Fang RH, et al. (2016). Nanoparticles camouflaged in platelet membrane coating as an antibody decoy for the treatment of immune thrombocytopenia. *Biomaterials* 111:116–23.
- Wei XL, Ying M, Dehaini D, et al. (2018). Nanoparticle functionalization with platelet membrane enables multifactorial biological targeting and detection of atherosclerosis. *ACS Nano* 12:109–16.
- Wu H, Jiang X, Li Y, et al. (2020). Engineering stem cell derived biomimetic vesicles for versatility and effective targeted delivery. *Adv Funct Mater* 30:2006169.
- Wu HH, Zhou Y, Tabata Y, et al. (2019a). Mesenchymal stem cell-based drug delivery strategy: from cells to biomimetic. *J Control Release* 294:102–13.
- Wu PY, Yin DT, Liu JM, et al. (2019b). Cell membrane based biomimetic nanocomposites for targeted therapy of drug resistant EGFR-mutated lung cancer. *Nanoscale* 11:19520–8.
- Wu XY, Li YC, Raza F, et al. (2021). Red blood cell membrane-camouflaged tedizolid phosphate-loaded PLGA nanoparticles for bacterial-infection therapy. *Pharmaceutics* 13:99.
- Xiao L, Huang Y, Yang YH, et al. (2021). Biomimetic cytomembrane nanovaccines prevent breast cancer development in the long term. *Nanoscale* 13:3594–601.
- Xie XT, Wang HJ, Williams GR, et al. (2019). Erythrocyte membrane cloaked curcumin-loaded nanoparticles for enhanced chemotherapy. *Pharmaceutics* 11:429.
- Xiong X, Zhao JY, Su R, et al. (2021). Double enhancement of immunogenic cell death and antigen presentation for cancer immunotherapy. *Nano Today* 39:101225.
- Xu C, Liu W, Hu Y, et al. (2020). Bioinspired tumor-homing nanopatform for co-delivery of paclitaxel and siRNA-E7 to HPV-related cervical malignancies for synergistic therapy. *Theranostics* 10:3325–39.
- Xu HG, Wang B, Ono M, et al. (2019). Targeted disruption of HLA genes via CRISPR-Cas9 generates iPSCs with enhanced immune compatibility. *Cell Stem Cell* 24:566–78.
- Xu LL, Chen YH, Jin QF, et al. (2021). Biomimetic PLGA microbubbles coated with platelet membranes for early detection of myocardial ischaemia-reperfusion injury. *Mol Pharm* 18:2974–85.
- Yaman S, Ramachandramoorthy H, Oter G, et al. (2020). Melanoma peptide MHC specific TCR expressing T-cell membrane camouflaged PLGA nanoparticles for treatment of melanoma skin cancer. *Front Bioeng Biotechnol* 8:943:943.
- Yang L, Zang GC, Li JW, et al. (2020). Cell-derived biomimetic nanoparticles as a novel drug delivery system for atherosclerosis: predecessors and perspectives. *Regen Biomater* 7:349–58.
- Yang N, Ding YP, Zhang YL, et al. (2018). Surface functionalization of polymeric nanoparticles with umbilical cord-derived mesenchymal stem cell membrane for tumor-targeted therapy. *ACS Appl Mater Interfaces* 10:22963–73.
- Yarousovsky M, Plyushch M, Popov D, et al. (2013). Prognostic value of endotoxin activity assay in patients with severe sepsis after cardiac surgery. *J Inflamm* 10:8.
- Ye H, Wang KY, Lu Q, et al. (2020). Nanosponges of circulating tumor-derived exosomes for breast cancer metastasis inhibition. *Biomaterials* 242:119932.
- Zhang C, Zhang W, Zhu DS, et al. (2022a). Nanoparticles functionalized with stem cell secretome and CXCR4-overexpressing endothelial membrane for targeted osteoporosis therapy. *J Nanobiotechnol* 20:35.
- Zhang L, Zhao W, Huang JK, et al. (2022b). Development of a dendritic cell/tumor cell fusion cell membrane nano-vaccine for the treatment of ovarian cancer. *Front Immunol* 13:828263.
- Zhang QZ, Dehaini D, Zhang Y, et al. (2018a). Neutrophil membrane-coated nanoparticles inhibit synovial inflammation and alleviate joint damage in inflammatory arthritis. *Nat Nanotechnol* 13:1182–90.
- Zhang QZ, Honko A, Zhou JR, et al. (2020a). Cellular nanosponges inhibit SARS-CoV-2 infectivity. *Nano Lett* 20:5570–4.

- Zhang XM, Ai FY, Li XY, et al. (2015). Inflammation-induced S100A8 activates Id3 and promotes colorectal tumorigenesis. *Int J Cancer* 137:2803–14.
- Zhang YT, He ZH, Li YY, et al. (2021). Tumor cell membrane-derived nano-Trojan horses encapsulating phototherapy and chemotherapy are accepted by homologous tumor cells. *Mater Sci Eng C Mater Biol Appl* 120:111670.
- Zhang Z, Qian HQ, Huang J, et al. (2018b). Anti-EGFR-iRGD recombinant protein modified biomimetic nanoparticles loaded with gambogic acid to enhance targeting and antitumor ability in colorectal cancer treatment. *Int J Nanomedicine* 13:4961–75.
- Zhang Z, Qian HQ, Yang M, et al. (2017). Gambogic acid-loaded biomimetic nanoparticles in colorectal cancer treatment. *Int J Nanomedicine* 12:1593–605.
- Zhang ZQ, Li D, Li XH, et al. (2020b). PEI-modified macrophage cell membrane-coated PLGA nanoparticles encapsulating Dendrobium polysaccharides as a vaccine delivery system for ovalbumin to improve immune responses. *Int J Biol Macromol* 165:239–48.
- Zheng XL, Huang YZ, Zheng CH, et al. (2010). Alginate-chitosan-PLGA composite microspheres enabling single-shot hepatitis B vaccination. *AAPS J* 12:519–24.
- Zheng XL, Zhu Y, Fei WD, et al. (2022). Redox-responsive and electrically neutral PLGA nanoparticles for siRNA delivery in human cervical carcinoma cells. *J Pharm Innov.*
- Zhong SS, Li LX, Shen X, et al. (2019). An update on lipid oxidation and inflammation in cardiovascular diseases. *Free Radic Biol Med* 144:266–78.
- Zhou H, Fan ZY, Lemons PK, et al. (2016). A facile approach to functionalize cell membrane-coated nanoparticles. *Theranostics* 6:1012–22.
- Zhu JH, Qin FH, Ji ZH, et al. (2019). Mannose-modified PLGA nanoparticles for sustained and targeted delivery in hepatitis B virus immunoprophylaxis. *AAPS Pharmscitech* 21:13.
- Zuo H, Qiang J, Wang Y, et al. (2022). Design of red blood cell membrane-cloaked dihydroartemisinin nanoparticles with enhanced antimalarial efficacy. *Int J Pharm* 618:121665.